

A tensor network approach to 2D bosonization

Sujeet K. Shukla, Tyler D. Ellison, and Lukasz Fidkowski
Department of Physics, University of Washington Seattle, USA 98105
 (Dated: February 19, 2024)

We present a 2D bosonization duality using the language of tensor networks. Specifically, we construct a tensor network operator (TNO) that implements an exact 2D bosonization duality. The primary benefit of the TNO is that it allows for bosonization at the level of quantum states. Thus, we use the TNO to provide an explicit algorithm for bosonizing fermionic projected entangled pair states (fPEPs). A key step in the algorithm is to account for a choice of spin-structure, encoded in a set of bonds of the bosonized fPEPS. This enables our tensor network approach to bosonization to be applied to systems on arbitrary triangulations of orientable 2D manifolds.

CONTENTS

I. Introduction	1	B. Calculation of the Koszul sign for a single loop	23
II. \mathbb{Z}_2 -graded tensor networks	2	C. Tensor Network Bosonization in 1D	24
A. \mathbb{Z}_2 -graded Hilbert spaces	3	1. Review of 1D bosonization	24
B. \mathbb{Z}_2 -graded tensors	3	2. TNO representation of the duality	25
C. Contraction map and tensor action	4	D. Bosonization of fermionic matrix product states	26
D. \mathbb{Z}_2 -graded representation of a fermionic operator algebra	4	1. Boundary conditions in 1D	26
E. \mathbb{Z}_2 -graded tensor network diagrams	5	2. Converting virtual indices to bosonic indices	28
III. Tensor network bosonization duality in 2D	5	3. Examples	29
A. Review of the operator-level bosonization duality	6	References	30
B. TNO representation of the 2D duality	7		
C. Bosonization of quantum states	10		
IV. Bosonization of fPEPS	11		
A. Contracting the bosonization TNO with an fPEPS	11		
B. Koszul signs and removable grading	11		
C. Koszul signs in the bosonized fPEPS	12		
1. Simplifying the Koszul sign calculation	12		
2. Contraction of basis tensors	13		
3. Basis contraction and cohomology	13		
4. Koszul signs from a single loop	14		
5. Winding number and Koszul signs	14		
D. Removing grading and choosing spin-structure	16		
1. Reproducing Koszul signs for contractible loops	16		
2. Reproducing Koszul signs for non-contractible loops	16		
3. General triangulation of a torus	18		
4. Higher genus manifolds	18		
5. Grading removal for the bosonized fPEPS	19		
E. Algorithm for bosonizing an fPEPS	19		
F. Example of bosonizing an fPEPS	20		
V. Conclusion and future work	21		
A. \mathbb{Z}_2 -graded tensor representation of Majorana operators	21		

I. INTRODUCTION

The Jordan-Wigner transformation is a well established example of a bosonization duality – it maps a system of spinless complex fermions to a system of spins [1]. The duality has led to many fruitful applications to one dimensional systems, where it equates 1D fermionic models and spin chains. However, while the Jordan-Wigner transformation is a powerful tool in one dimension, there are challenges to applying it to higher dimensional systems. To implement the Jordan-Wigner transformation in dimensions greater than one, the duality is applied along a 1D path which snakes through the fermionic system. In general, this yields a transformation that maps local fermionic Hamiltonians to *non*-local bosonic Hamiltonians.

Generalizations of the Jordan Wigner transformation to two dimensions have since overcome this obstacle and indeed map local fermionic Hamiltonians to local bosonic Hamiltonians [2,3,4,5]. Similar to the one dimensional Jordan-Wigner transformation, these two dimensional bosonization dualities are expressed at the level of operators. That is, they define a mapping of operators, where operators that act on fermionic degrees of freedom are mapped to operators that act on spins. Such a mapping of operators⁶ necessarily comes from conjugating by some unitary operator on the Hilbert space [7]. However, finding the explicit form of this unitary, and thereby obtaining the action of the duality at the level of quantum states, is challenging.

In this work, we formulate a two dimensional bosonization duality at the level of quantum states. Specifically, we identify a tensor network representation of the duality in Ref. [2]. This is to say, we construct a tensor network operator (TNO) which, by conjugation, maps operators according to the transformation in Ref. [2]. Moreover, the TNO may be applied directly to fermionic tensor network states to map them to bosonic states. Further, we show that bosonized fermionic projected entangled pair states (fPEPS) may be written explicitly as bosonic projected entangled pair states (bPEPS).

The TNO inherits two of the main features of the transformation detailed in Ref. [2]. First, the mapping of operators in Ref. [2] makes the physical interpretation of two dimensional bosonization transparent – fermionic excitations are mapped to *emergent* fermions in a \mathbb{Z}_2 gauge theory. Operators that create pairs of fermions are explicitly mapped to operators that create pairs of emergent fermions, which are interpreted as bound states of a bosonic gauge charge and flux. The gauge constraint on the bosonic side of the duality expressly prohibits unbound charge and flux excitations. Consequently, our TNO clearly maps the subspace of states with an even number of fermions to a constrained Hilbert space with a basis given by configurations of emergent fermions. Second, the bosonization duality of Ref. [2] carefully accounts for spin-structure – a mathematical input necessary for bosonization dualities – while in other treatments, spin-structure is hidden in seemingly arbitrary choices. In our construction, a choice of spin-structure is then specified by a certain set of bonds in the TNO. Importantly, keeping track of the spin-structure allows us to establish our tensor network bosonization for fermionic systems on arbitrary triangulations of closed, orientable 2D manifolds.

For context, our approach to bosonization is analogous to a method employed in Ref. [8] for gauging symmetries at the level of quantum states. In Ref. [8], a TNO is used to map a state with a global symmetry to a state with the corresponding gauge symmetry. Indeed, symmetries may be gauged by using a duality [9], and the TNOs in Ref. [8] can be understood as a tensor network representation of the duality corresponding to gauging the symmetry. We note that, using the methods of Ref. [8] to gauge the fermion parity symmetry in a fermionic system, one obtains a TNO that is closely related to our bosonization TNO. However, unlike the bosonization TNO, the TNO corresponding to gauging fermion parity maps to a system with fermionic degrees of freedom (although, see [10]). The inverse (or Hermitian conjugate) of our bosonization TNO (this maps a bosonic state to a fermionic state) can be understood as “un-gauging” fermion parity or “fermion condensation” [11,12,13].

We emphasize that our bosonization duality is distinct from the efforts to express fermionic tensor networks in terms of bosonic tensor networks. Refs. [14,15,16] develop strategies for rewriting fermionic tensor net-

work states as bosonic tensor network states. However, these do not change the state – only its tensor network representation. The bosonization duality, in contrast, maps unentangled fermionic states to long-range entangled bosonic states. Nonetheless, our bosonization duality may prove useful for analyzing fermionic states, since expectation values of local fermionic operators can be recovered by computing the expectation value of the transformed operators in the bosonized tensor network state. Furthermore, our bosonization duality and the subsequent rewriting as an explicit bosonic tensor network state preserves the locality of the tensor network and only increases the bond dimension by a factor of 2.

The remainder of the paper is structured as follows. We begin by introducing the formalism of \mathbb{Z}_2 -graded Hilbert spaces and \mathbb{Z}_2 -graded tensor networks. We find the language of \mathbb{Z}_2 -graded tensor networks especially convenient for expressing our bosonization TNO, and we use the notation established in section II throughout the text. We encourage readers that are familiar with the formalism of \mathbb{Z}_2 -grading to briefly skim section II to simply acquaint themselves with our notation. Before constructing the bosonization TNO, we review the 2D bosonization duality of Ref. [2], in section III A. Subsequently, in section III B we construct the TNO that implements this 2D bosonization duality at the level of states. After applying the bosonization TNO to a fermionic tensor network state, the resulting state is not explicitly a bosonic tensor network state. Therefore, section IV is devoted to describing an algorithmic procedure for “removing the grading” and rewriting a bosonized fPEPS as a bPEPS. The procedure involves summing over inequivalent spin-structures, discussed in section IV D. Lastly, we note that we describe a tensor network representation of 1D bosonization in Appendices C and D.

II. \mathbb{Z}_2 -GRADED TENSOR NETWORKS

Our bosonization TNO is naturally expressed in terms of \mathbb{Z}_2 -graded tensor networks. Therefore, the purpose of this section is to give a concise introduction to \mathbb{Z}_2 -graded tensor networks and establish the notation used throughout the text. For a similar exposition of \mathbb{Z}_2 -graded tensor networks, one can consult Refs. [17,18]. We start by defining \mathbb{Z}_2 -graded Hilbert spaces and \mathbb{Z}_2 -graded tensors. Then, we introduce the contraction map to “glue” together \mathbb{Z}_2 -graded tensors. The contraction map allows us to define a linear action of tensors on each other and to form \mathbb{Z}_2 -graded tensor networks. Accordingly, we describe a representation of a fermionic operator algebra in terms of \mathbb{Z}_2 -graded tensors and present a diagrammatic representation for \mathbb{Z}_2 -graded tensor networks.

A. \mathbb{Z}_2 -graded Hilbert spaces

A \mathbb{Z}_2 -graded Hilbert space is a Hilbert space \mathcal{H} with a natural direct sum decomposition: $\mathcal{H} = \mathcal{H}^0 \oplus \mathcal{H}^1$. A vector $|j\rangle \in \mathcal{H}$ lying solely in either \mathcal{H}^0 or \mathcal{H}^1 has a $\{0, 1\}$ valued *grading* denoted as $|j|$, where $|j| = 0$ if $|j\rangle \in \mathcal{H}^0$ and $|j| = 1$ if $|j\rangle \in \mathcal{H}^1$. (We use round brackets for vectors in \mathbb{Z}_2 -graded Hilbert spaces.) In the context of fermionic systems, we consider \mathcal{H}^0 to be the subspace spanned by states with an even number of fermions and \mathcal{H}^1 to be the subspace spanned by states with an odd number of fermions. Thus, the grading of a vector and its fermion parity coincide. For this reason, we use grading and parity interchangeably. Further, we refer to vectors with a definite parity as homogeneous vectors, and we call states formed from a superposition of both even and odd parity vectors inhomogeneous.

To capture the physics of a many-body fermionic system, we will need a generalization of the usual tensor product – the graded tensor product $\hat{\otimes}$. For graded Hilbert spaces \mathcal{H}_a and \mathcal{H}_b , we define the graded tensor product space $\mathcal{H}_a \hat{\otimes} \mathcal{H}_b$ to be the quotient space:

$$\mathcal{H}_a \hat{\otimes} \mathcal{H}_b \equiv \frac{(\mathcal{H}_a \otimes \mathcal{H}_b) \oplus (\mathcal{H}_b \otimes \mathcal{H}_a)}{\sim}. \quad (1)$$

Here, \otimes is the usual (unsymmetrized) tensor product of Hilbert spaces, and \sim denotes the relation:

$$|j\rangle_a \otimes |k\rangle_b \sim (-1)^{|j||k|} |k\rangle_b \otimes |j\rangle_a \quad (2)$$

for $|j\rangle_a \in \mathcal{H}_a$ and $|k\rangle_b \in \mathcal{H}_b$ both with definite grading. The Hilbert space $\mathcal{H}_a \hat{\otimes} \mathcal{H}_b$ is itself a graded Hilbert space with the equivalence class $|j\rangle_a \hat{\otimes} |k\rangle_b \in \mathcal{H}_a \hat{\otimes} \mathcal{H}_b$ having a grading of $|j| + |k| \bmod 2$. As a consequence of Eq. (2), we have:

$$|j\rangle_a \hat{\otimes} |k\rangle_b = (-1)^{|j||k|} |k\rangle_b \hat{\otimes} |j\rangle_a. \quad (3)$$

This property of the graded tensor product is key to describing fermions, as it encodes the exchange statistics of the fermions. One can see that the graded tensor product captures the familiar notion of a fermionic Fock space by representing the equivalence class $|j\rangle_a \hat{\otimes} |k\rangle_b$ by the vector $\frac{1}{2}(|j\rangle_a \otimes |k\rangle_b + (-1)^{|j||k|} |k\rangle_b \otimes |j\rangle_a)$. When $|j\rangle_a$ and $|k\rangle_b$ are both fermion parity odd, we have an anti-symmetric combination – the Slater determinant.

Before moving on to describe \mathbb{Z}_2 -graded tensors, we would like to note that Hilbert spaces for bosonic systems also fit into the framework of \mathbb{Z}_2 -graded Hilbert spaces. A bosonic Hilbert space can be understood as a \mathbb{Z}_2 -graded Hilbert space for which \mathcal{H}^1 , the space of vectors with odd grading, is empty, leaving $\mathcal{H} = \mathcal{H}^0$. The graded tensor product between two bosonic Hilbert spaces reduces to the symmetrized tensor product between the Hilbert spaces, as is standard in tensor networks for bosonic systems. In a slight abuse of notation, we will denote vectors $|j\rangle$ in bosonic Hilbert spaces with angled brackets. In what follows, we will freely take graded tensor products

of states in bosonic Hilbert spaces and states in fermionic Hilbert spaces, and the angled brackets are to remind us that those vectors necessarily have trivial grading.

B. \mathbb{Z}_2 -graded tensors

A rank N \mathbb{Z}_2 -graded tensor T is an element of the graded tensor product of N \mathbb{Z}_2 -graded Hilbert spaces, i.e., $\mathsf{T} \in \mathcal{H}_1 \hat{\otimes} \dots \hat{\otimes} \mathcal{H}_N$. Similar to tensors used to study bosonic systems, \mathbb{Z}_2 -graded tensors admit a convenient graphical representation. Let us consider a specific example with $N = 4$ for illustration:

$$\begin{array}{c} s \\ \downarrow \\ \boxed{\mathsf{T}} \\ \uparrow \\ q \end{array} \quad \begin{array}{c} r \rightarrow \\ \leftarrow p \end{array} \quad \equiv \quad \sum_{a,b,c,d} T_{abcd} |a\rangle_p |b\rangle_q \langle c|_r \langle d|_s. \quad (4)$$

On the left hand side of Eq. (4), we have a diagrammatic representation of the tensor $\mathsf{T} \in \mathcal{H}_p \hat{\otimes} \mathcal{H}_q \hat{\otimes} \mathcal{H}_r^* \hat{\otimes} \mathcal{H}_s^*$, where \mathcal{H}^* is the dual Hilbert space of \mathcal{H} . In the diagram, the characters at the end of the legs label the Hilbert spaces, and the orientation of the leg indicates whether we consider the Hilbert space to be a dual Hilbert space. (Legs oriented towards the node correspond to a dual Hilbert space.) Further, we have used red legs for \mathbb{Z}_2 -graded Hilbert spaces and black legs for bosonic Hilbert spaces.

The right hand side of Eq. (4) is the tensor component form of T with *component values* T_{abcd} . Note that we have suppressed the $\hat{\otimes}$ between vectors, and as previously mentioned, we use angled brackets for vectors which necessarily have trivial grading [$\langle c|_r$ in Eq. (4)]. Thus, the vector $|a\rangle_p |b\rangle_q \langle c|_r \langle d|_s$ has a grading of $|a| + |b| + |d| \bmod 2$. Since the graded tensor product of Hilbert spaces is a graded Hilbert space, a tensor can be either homogeneous or inhomogeneous. A homogeneous tensor has nonzero component values only for vectors sharing the same parity, and otherwise, the tensor is inhomogeneous.

It is important to note that the tensor T is independent of the ordering of vectors in Eq. (4), but the component values (T_{abcd}) can depend on the ordering. For example, if we swap the order of $|a\rangle_p$ and $|b\rangle_q$, we get:

$$\mathsf{T} = \sum_{a,b,c,d} T_{abcd} (-1)^{|a||b|} |b\rangle_q |a\rangle_p \langle c|_r \langle d|_s. \quad (5)$$

Hence, the tensor components have an additional sign $(-1)^{|a||b|}$ with the new choice of ordering. The ordering should therefore be interpreted as a particular choice of orthonormal basis with which to express the tensor. We will often refer to the choice of ordering of the vectors in the component form of a tensor as a choice of *internal ordering*.

then the creation and annihilation operators have the following canonical representations:

$$\begin{aligned} c_p|1\rangle_p &= |0\rangle_p, \quad c_p|0\rangle_p = 0 \\ c_p^\dagger|1\rangle_p &= 0, \quad c_p^\dagger|0\rangle_p = |1\rangle_p. \end{aligned} \quad (15)$$

Using Eq. (11), this leads to the following representation of Majorana operators:

$$p \leftarrow \textcircled{\gamma} \leftarrow p \equiv |1\rangle_p \langle 0|_p + |0\rangle_p \langle 1|_p \quad (16)$$

$$= \sum_a |a+1\rangle_p \langle a|_p$$

$$p \leftarrow \textcircled{\bar{\gamma}} \leftarrow p \equiv i|1\rangle_p \langle 0|_p - i|0\rangle_p \langle 1|_p \quad (17)$$

$$= \sum_a (-1)^a i|a+1\rangle_p \langle a|_p.$$

Here, and throughout the paper, indices are assumed to take binary values, unless stated otherwise. Thus, $\sum_a \equiv \sum_{a=0}^1$, and $(a+1) \equiv (a+1) \bmod 2$, etc. In Appendix A, we show that the algebraic properties of the Majorana operators are indeed satisfied by the tensor representations in Eqs. (16) and (17). Furthermore, using Eq. (14), fermion parity P can be represented as:

$$\begin{aligned} p \leftarrow \textcircled{P} \leftarrow p &\equiv \sum_a (-1)^a |a\rangle_p \langle a|_p \\ &= |0\rangle_p \langle 0|_p - |1\rangle_p \langle 1|_p. \end{aligned} \quad (18)$$

Eq. (18) agrees with the intuition that the \mathbb{Z}_2 -grading of a vector corresponds to the fermion parity of the state.

E. \mathbb{Z}_2 -graded tensor network diagrams

To establish a general theory of \mathbb{Z}_2 -graded tensor networks, we need to make sure that tensor diagrams can unambiguously represent the algebraic values. For example, given the tensor network diagram:

$$\begin{array}{c} \downarrow \\ \textcircled{A} \leftarrow \textcircled{B} \leftarrow \textcircled{C} \end{array}, \quad (19)$$

how do we know whether it represents the tensor $A \cdot B \cdot C$ or $B \cdot C \cdot A$, or any other order of action of tensors A , B , and C ? Unlike bosonic tensors, \mathbb{Z}_2 -graded tensors do not commute with each other, and hence, in general, $A \cdot B \cdot C$ and $B \cdot C \cdot A$ are different tensors. If T and S are homogeneous tensors, then the commutation relation of graded tensor products in Eq. (3) implies the following commutation relation:

$$T \cdot S = (-1)^{|T||S|} S \cdot T. \quad (20)$$

In particular, as long as only one tensor is odd, we have $T \cdot S = S \cdot T$, and the order of action of these tensors does not matter. Extending this argument, we see that for a

set of homogeneous tensors $\{A, B, C, \dots\}$, as long as at most one tensor is odd, the order of contraction does not matter.

What happens when more than one odd tensor appears in a TN? An example of such a tensor network is given in the following diagram, where we assume A is an even tensor:

$$\begin{array}{c} \downarrow \\ \textcircled{\gamma} \rightarrow \textcircled{A} \leftarrow \textcircled{\bar{\gamma}} \end{array}. \quad (21)$$

How should this tensor network diagram be read algebraically? For instance, it could represent either $\gamma \cdot A \cdot \bar{\gamma}$ or $\bar{\gamma} \cdot \gamma \cdot A$, among other possibilities. This is problematic because, according to Eq. (20), $\gamma \cdot A \cdot \bar{\gamma} = -\bar{\gamma} \cdot \gamma \cdot A$. Hence, the algebraic value of this tensor network diagram is ill defined.

To remove this ambiguity, we need to indicate the order in which γ and $\bar{\gamma}$ are applied. We do this by adopting the following simple notation: if two or more odd tensors appear in a diagram, we place numbers next to their nodes to indicate their relative order. For example, $\gamma \cdot A \cdot \bar{\gamma}$ and $\bar{\gamma} \cdot \gamma \cdot A$ are then respectively represented by the following diagrams:

$$\begin{aligned} \gamma \cdot A \cdot \bar{\gamma} &\equiv \begin{array}{c} \downarrow \\ \textcircled{\gamma} \rightarrow \textcircled{A} \leftarrow \textcircled{\bar{\gamma}} \\ \quad 2 \qquad \qquad 1 \end{array} \\ \bar{\gamma} \cdot \gamma \cdot A &\equiv \begin{array}{c} \downarrow \\ \textcircled{\gamma} \rightarrow \textcircled{A} \leftarrow \textcircled{\bar{\gamma}} \\ \quad 1 \qquad \qquad 2 \end{array}. \end{aligned} \quad (22)$$

In fact, the first diagram can also represent any tensor network in which $\bar{\gamma}$ is applied *before* γ , so it can also represent $\gamma \cdot \bar{\gamma} \cdot A$ or $A \cdot \gamma \cdot \bar{\gamma}$. Similarly, the second diagram can also represent $\bar{\gamma} \cdot A \cdot \gamma$ and $A \cdot \bar{\gamma} \cdot \gamma$ (recall that we assume A is an even tensor).

III. TENSOR NETWORK BOSONIZATION DUALITY IN 2D

In this section, we use the formalism of \mathbb{Z}_2 -graded tensor networks to construct a TNO that implements the exact 2D bosonization duality of Ref. [2]. We start by reviewing the operator-level duality, and then show that it can be naturally represented by a TNO, which we refer to as the bosonization TNO. The TNO representation allows us to easily compute the action of bosonization on quantum states (as opposed to just the action on operators). In particular, in section IV, we use the bosonization TNO to map fermionic tensor network states to bosonic tensor network states.

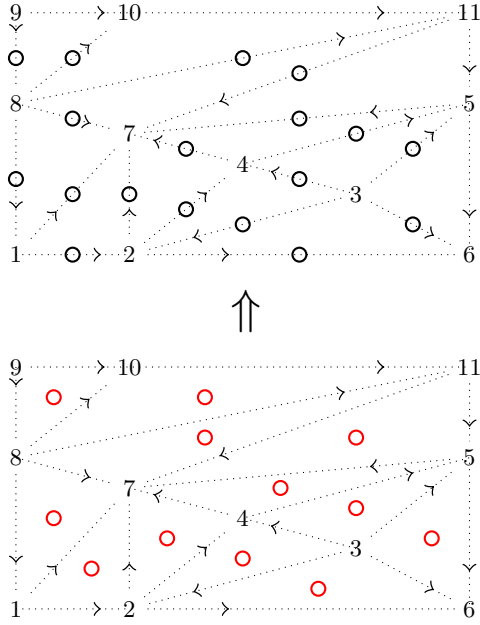


FIG. 1. The bosonization duality maps a system of spinless complex fermions to a system of spin-1/2 degrees of freedom. The bottom picture shows the fermionic degrees of freedom (red circles) at each triangular face f . The top picture shows the spin-1/2 bosonic degrees of freedom (black circles) on each edge e .

A. Review of the operator-level bosonization duality

To begin, we describe the lattice on which the duality is defined and set some notation. The duality in Ref. [2] can be defined on an arbitrary triangulation of a 2D manifold with boundary [11,19]. It is also required that the lattice has a branching structure, i.e. each edge has an orientation (see Fig. 1) such that the edges around any triangle do not form a cycle. The branching structure yields an ordering of the vertices around a triangle and allows us to define an orientation of each triangle relative to the orientation of the underlying oriented manifold. We denote the ordered vertices of the triangular face f as f_0, f_1 and f_2 , where f_j is the j -vertex of the triangle, and j refers to the number of edges of the triangle f that point toward f_j . We adopt the convention that a triangle is positively oriented if f_0, f_1 and f_2 appear in counter-clockwise order, and otherwise it is negatively oriented. Further, we label the edges of f by f_{01}, f_{12} , and f_{02} , such that f_{jk} is the edge pointing from f_j to f_k . We also find it convenient to denote the endpoints of the edge e as e_0 and e_1 , with e pointing from e_0 to e_1 .

Let us illustrate the notation above using examples from Fig. 1. (Note that the vertices in Fig. 1 are labeled with integers arbitrarily simply to guide the discussion. They do not denote a global ordering of the vertices.) If $f = \langle 3, 2, 4 \rangle$ then $f_0 = \langle 3 \rangle, f_1 = \langle 2 \rangle, f_2 = \langle 4 \rangle$ and $f_{01} = \langle 3, 2 \rangle, f_{12} = \langle 2, 4 \rangle, f_{02} = \langle 3, 4 \rangle$. Further, if $e = \langle 2, 4 \rangle$,

then $e_0 = 2, e_1 = 4$. The triangle $\langle 8, 1, 7 \rangle$ is positively oriented while $\langle 3, 2, 4 \rangle$ is negatively oriented.

We are now in a position to describe the fermionic degrees of freedom on the lattice and the corresponding operator algebra mapped by the bosonization duality. Each triangle f hosts a spinless complex fermion, and as explained in section IID, its operator algebra is generated by Majorana operators, γ_f and $\bar{\gamma}_f$. The total fermionic algebra is generated by the set of $\gamma_f, \bar{\gamma}_f$ for all triangles f .

The bosonization duality is defined on a subset of the full fermionic operator algebra to ensure that the duality maps local operators to local operators. Specifically, the duality is defined on the subalgebra of even operators \mathcal{E} , i.e., the operators that commute with the global fermion parity operator $\prod_f P_f$, where

$$P_f = -i\gamma_f\bar{\gamma}_f \quad (23)$$

is the fermion parity operator at f . \mathcal{E} is generated by fermion parity P_f at each triangle f , and *hopping operators* S_e at each edge e defined as:

$$S_e = i(-1)^{\eta_e}\gamma_{L_e}\bar{\gamma}_{R_e}. \quad (24)$$

Here, L_e and R_e denote the triangle to the left and right of the edge e , respectively. For example, in Fig. 1, we have $L_{\langle 2, 4 \rangle} = \langle 2, 4, 7 \rangle$ and $R_{\langle 2, 4 \rangle} = \langle 3, 2, 4 \rangle$. $(-1)^{\eta_e}$ is a sign that comes from a choice of the so-called *spin-structure* η [11]. We postpone a detailed discussion of spin-structure until section IVD below. For now, η should be understood as a chosen set of edges with η_e defined as:

$$\eta_e = \begin{cases} 1 & \text{if } e \in \eta \\ 0 & \text{otherwise.} \end{cases} \quad (25)$$

As we will explain below, η is dependent upon the branching structure, and roughly speaking, ensures that the bosonization duality is uniform across the 2D manifold.

We now discuss the relations satisfied by the generators of the even algebra \mathcal{E} . First, all parity operators commute with each other: $P_f P_{f'} = P_{f'} P_f$, for all f, f' . However, not all hopping operators commute with each other. Instead, they satisfy the following commutation relations:

$$S_e S_{e'} = (-1)^{\delta_{L_e, L_{e'}}} (-1)^{\delta_{R_e, R_{e'}}} S_{e'} S_e. \quad (26)$$

That is, two hopping operators anticommute if and only if they have a common triangle to the left or to the right. For example, in Fig. 1, $S_{\langle 2, 4 \rangle}$ and $S_{\langle 3, 2 \rangle}$ anticommute because they have a common triangle to the right: $R_{\langle 2, 4 \rangle} = R_{\langle 3, 2 \rangle} = \langle 3, 2, 4 \rangle$. However, $S_{\langle 2, 4 \rangle}$ and $S_{\langle 3, 4 \rangle}$ commute because they do not have a common right or left triangle. Parity operators and hopping operators anticommute if they share a triangle:

$$S_e P_f = (-1)^{\delta_{e \subset f}} P_f S_e, \quad (27)$$

otherwise they commute. ($\delta_{e \subset f} = 1$ if edge e is part of the triangle, otherwise it is 0.) Furthermore, the fermion parity operators and hopping operators are not independent, since for each vertex v , they satisfy the relation [11]:

$$\prod_{e: e_0=v} S_e \prod_{e: e_1=v} S_e \prod_{f: f_0, f_2=v} P_f = 1. \quad (28)$$

In equation (28), the first product is over all edges e for which the e_0 vertex is v , the second product is over all edges e for which v is the e_1 vertex, and the last product is over all triangles for which v is either a 0-vertex or a 2-vertex. Note that the sign of $(-1)^{\eta_e}$ in the definition of the hopping operator [Eq. (24)] is crucial to obtain 1 on the right hand side of Eq. (28). This completes our description of the algebra \mathcal{E} on the fermionic side of the duality²⁰, and we move on to describe the bosonic side of the duality.

On the bosonic side of the duality, as shown in Fig. 1, we have a spin-1/2 degree of freedom at each edge e . The operator algebra at e is generated by the Pauli operators X_e and Z_e , and the full bosonic algebra is generated by the set containing X_e and Z_e for all edges e . The bosonization duality maps to just a subalgebra of the full bosonic algebra, where the subalgebra is defined by a certain \mathbb{Z}_2 gauge constraint. The explicit form for the gauge constraint will emerge naturally from the mapping of operators described below.

The bosonization duality \mathfrak{D} , is a homomorphism from the algebra of fermion parity even operators \mathcal{E} to a particular bosonic subalgebra. \mathfrak{D} is defined by its action on the generators of \mathcal{E} , P_f and S_e . It maps fermion parity P_f to an operator that measures the \mathbb{Z}_2 flux at triangle f , namely:

$$W_f \equiv Z_{f_{01}} Z_{f_{12}} Z_{f_{02}}. \quad (29)$$

Since S_e and P_f anticommute whenever e borders f , a natural first guess for the image of S_e under \mathfrak{D} is the operator X_e . X_e creates a pair of \mathbb{Z}_2 fluxes and hence anti-commutes with the operator that measures flux on a neighboring triangle. However, mapping S_e to X_e does not preserve the commutation relations with the other hopping operators. To remedy this, we dress X_e with Pauli Z operators:

$$U_e \equiv X_e \prod_{f \in \{L_e, R_e\}} Z_{f_{01}}^{\delta_{e, f_{12}}}. \quad (30)$$

In words, the expression in Eq. (30) says that if e is the f_{12} edge of the triangle to the left, then we include a factor of $Z_{f_{01}}$ on the f_{01} edge of that triangle. Likewise, if e is the f_{12} edge of the triangle to the right, then we include a factor of $Z_{f_{01}}$ on the f_{01} edge of that triangle. For example, looking at Fig. 1, we have $U_{\langle 3,4 \rangle} = X_{\langle 3,4 \rangle}$, $U_{\langle 2,4 \rangle} = X_{\langle 2,4 \rangle} Z_{\langle 3,2 \rangle}$, $U_{\langle 5,7 \rangle} = X_{\langle 2,7 \rangle} Z_{\langle 4,5 \rangle} Z_{\langle 11,5 \rangle}$, etc.

Lastly, we must check that the relation in Eq. (27) is preserved by the bosonization duality. For each vertex v ,

we find:

$$\prod_{e: e_0=v} U_e \prod_{e: e_1=v} U_e \prod_{f: f_0, f_2=v} W_f = G_v, \quad (31)$$

where G_v is equal to:

$$G_v = \prod_{e \supset v} X_e \prod_{f: f_0=v} W_f. \quad (32)$$

The first product in Eq. (32) is over all edges e connected to v . Thus, to preserve the relation (27), we need to impose the gauge constraint $G_v = 1$ for all v .

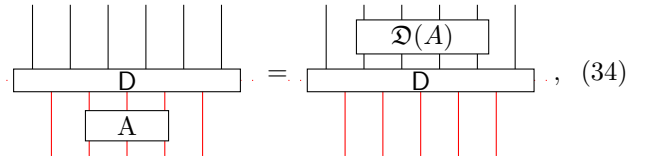
Denoting by \mathcal{G} the bosonic subalgebra generated by the set of W_f and U_e with the gauge constraint $G_v = 1$ for all v , we see that the 2D bosonization duality \mathfrak{D} is a bijective map from \mathcal{E} to \mathcal{G} defined by:

$$\begin{aligned} \mathfrak{D}(P_f) &= W_f, \\ \mathfrak{D}(S_e) &= U_e. \end{aligned} \quad (33)$$

The choice of spin-structure η ensures that the gauge constraint on the bosonic side of the duality is $G_v = 1$ at every vertex v . In section IV, we detail a prescription for choosing a suitable spin structure η .

B. TNO representation of the 2D duality

Having reviewed both \mathbb{Z}_2 -graded tensor networks and the operator-level 2D bosonization duality, we can now describe one of our main results – a realization of 2D bosonization at the level of quantum states. To accomplish this, we represent the bosonization duality \mathfrak{D} in Eq. (33) using a TNO, \mathbf{D} . We say that a TNO \mathbf{D} represents the duality \mathfrak{D} , if it satisfies:



$$\text{Diagram (34): } \mathbf{D} \text{ with } A \text{ on bottom lines} = \mathbf{D} \text{ with } \mathfrak{D}(A) \text{ on top lines}.$$

for all fermion parity even operators $A \in \mathcal{E}$. Algebraically, this is:

$$\mathbf{D} \cdot A = \mathfrak{D}(A) \cdot \mathbf{D}. \quad (35)$$

In Eq. (35), we have used the operation \cdot defined in section II C for the contraction of \mathbb{Z}_2 -graded tensors. For Eq. (35) to hold, it suffices to show that \mathbf{D} satisfies Eq. (35) for the generators of \mathcal{E} , since for any $A, B, C \in \mathcal{E}$ we have:

$$\begin{aligned} \mathbf{D} \cdot (AB + C) &= \mathbf{D} \cdot AB + \mathbf{D} \cdot C \\ &= \mathfrak{D}(A) \cdot \mathbf{D} \cdot B + \mathfrak{D}(C) \cdot \mathbf{D} \\ &= \mathfrak{D}(A) \mathfrak{D}(B) \cdot \mathbf{D} + \mathfrak{D}(C) \cdot \mathbf{D} \\ &= \mathfrak{D}(AB + C) \cdot \mathbf{D} \end{aligned} \quad (36)$$

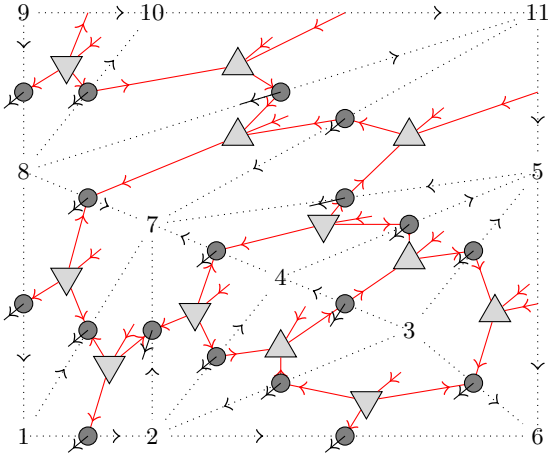


FIG. 2. TNO representation of the bosonization duality on a general triangulation of a 2D torus. The TNO is constructed from three types of tensors: F on positive triangles (downward pointing triangular nodes), \bar{F} on negative triangles (upward pointing triangular nodes), and B_η on edges (circular nodes). The TNO is a map from the fermionic legs (red legs, pointing towards the triangular nodes from behind) of F and \bar{F} tensors to the bosonic legs of B_η (black legs, pointing out of the page).

Hence, we need only find a D that satisfies:

$$D \cdot P_f = W_f \cdot D \quad (37a)$$

$$D \cdot S_e = U_e \cdot D, \quad (37b)$$

for all triangles f and edges e . To this end, we propose the TNO ansatz for D shown in Fig. 2.

The ansatz depicted in Fig. 2 is created by contracting together three kinds of tensors: tensors $F[f]$ on positively oriented triangles, tensors $\bar{F}[f]$ on negatively oriented triangles, and tensors $B_\eta[e]$ on edges. In explicit component form, the tensors $F[f]$ and $\bar{F}[f]$ are:

$$F[f] \equiv \sum_{j,a,b,c} F_{a,b,c}^j |c\rangle_{f_{01}} |a\rangle_{f_{12}} \langle b|_{f_{02}} \langle j|_f$$

$$\bar{F}[f] \equiv \sum_{j,a,b,c} \bar{F}_{a,b,c}^j |b\rangle_{f_{02}} \langle a|_{f_{12}} \langle c|_{f_{01}} \langle j|_f, \quad (38)$$

where all sums are over binary values. Diagrammatically, we represent $F[f]$ and $\bar{F}[f]$ respectively as:

$$F[f] \quad , \quad \bar{F}[f] \quad . \quad (39)$$

The legs labeled by f are the physical legs and extend into the page. These legs contract with fermionic operators or a fermionic tensor network state when the TNO is applied.

The tensor $B_\eta[e]$ at each edge is obtained by making a spin-structure dependent modification to a tensor $B[e]$.

$B[e]$ has the component form:

$$B[e] = \sum_{j,a,b} B_{a,b}^j |a\rangle_e |j\rangle_e \langle b|_e, \quad (40)$$

while the component form of $B_\eta[e]$ is:

$$B_\eta[e] = Z_e^{\eta_e} \cdot B$$

$$= \sum_{j,a,b} (-1)^{j\eta_e} B_{a,b}^j |a\rangle_e |j\rangle_e \langle b|_e, \quad (41)$$

which is pictorially represented as:

$$e \text{---} \text{dark node} \text{---} e \equiv e \text{---} \text{light node} \text{---} e. \quad (42)$$

The darker node on the left hand side represents B_η , and the lighter node on the right hand side represents B . The physical legs are bosonic Hilbert spaces depicted in black and pointing out of the page.

Now, we view the constraints in (37a) and (37b) as symmetries of the tensor D . These symmetries can be further reduced to symmetries of the local tensors of D , which then fixes the values of the local tensors. Indeed, we now show that D satisfies Eqs. (37a) and (37b), if the local tensors F , \bar{F} and B satisfy the symmetries depicted in Fig. 3. Algebraically, we write the symmetries for $F[f]$ and $\bar{F}[f]$ as:

$$F = P_{f_{01}} \cdot P_{f_{12}} \cdot F \cdot P_{f_{02}} \cdot P_f = P_{f_{01}} \cdot \gamma_{f_{12}} \cdot F \cdot \gamma_f$$

$$= \gamma_{f_{01}} \cdot F \cdot \gamma_f = F \cdot \gamma_{f_{02}} \cdot i\bar{\gamma}_f \quad (43)$$

$$\bar{F} = P_{f_{02}} \cdot \bar{F} \cdot P_{f_{01}} \cdot P_{f_{12}} \cdot P_f = \bar{F} \cdot \gamma_{f_{12}} \cdot P_{f_{01}} \cdot i\bar{\gamma}_f$$

$$= \bar{F} \cdot \gamma_{f_{01}} \cdot i\bar{\gamma}_f = \gamma_{f_{02}} \cdot \bar{F} \cdot \gamma_f \quad (44)$$

and the symmetries for $B[e]$ can be written as:

$$B_\eta = P_e \cdot B_\eta \cdot P_e = P_e \cdot Z_e \cdot B_\eta = (-1)^{\eta_e} \gamma_e \cdot X_e \cdot B_\eta \cdot \gamma_e, \quad (45)$$

where the contractions in Eqs. (43), (44), and (45) should be read in conjunction with the diagrams in Fig. 3. We note that the first symmetries of F , \bar{F} , and B imply that each of these tensors is fermion parity even.

To see how the symmetries of the local tensors ensure that D satisfies the relations in Eqs. (37a) and (37b) we use the graphical representations of the symmetries shown in Fig. 3. For example, consider the action of the

$$B[e] \propto \sum_a |a\rangle_e |a\rangle_e (a|_e. \quad (47)$$

Remember that all indices take values in $\{0, 1\}$, and $a + b + c \equiv a + b + c \pmod{2}$.

C. Bosonization of quantum states

We are now able to define the bosonization of quantum states, wherein a fermionic state is bosonized by simply applying the bosonization TNO. Before providing a simple example, we comment on constraints of the state-level duality that arise from the symmetries of D . In particular, we show that fermion parity odd states belong to the kernel of D and that D maps to bosonic states satisfying the constraint $G_v = 1$ for all v . Hence, fermion parity even states are mapped to bosonic states in a certain \mathbb{Z}_2 gauge theory.

To show that fermion parity odd states are in the kernel of the bosonization TNO, we use that $\prod_f W_f = 1$ on a closed manifold. This leads to:

$$D = \prod_f W_f \cdot D = D \cdot \prod_f P_f. \quad (48)$$

When D is applied to a fermionic state $|\psi_f\rangle$, Eq. (48) implies:

$$D|\psi_f\rangle = D \cdot \prod_f P_f |\psi_f\rangle. \quad (49)$$

Thus, if $|\psi_f\rangle$ is fermion parity odd, we have: $\prod_f P_f |\psi_f\rangle = -|\psi_f\rangle$, and it must be that $D|\psi_f\rangle = 0$.

The constraints on the image of D can be determined using the relation in Eq. (28). We see that:

$$\begin{aligned} D &= D \cdot \left(\prod_{e:e_0=v} S_e \prod_{e:e_1=v} S_e \prod_{f:f_0, f_2=v} P_f \right) \\ &= \left(\prod_{e:e_0=v} U_e \prod_{e:e_1=v} U_e \prod_{f:f_0, f_2=v} W_f \right) \cdot D \\ &= G_v \cdot D. \end{aligned}$$

Hence, for any bosonic state $\langle\psi_b|$:

$$\langle\psi_b|D = \langle\psi_b|G_v \cdot D, \quad (50)$$

which implies that D projects to the $G_v = 1$ subspace for each vertex v .

Now, we give a first example of the state-level duality and use the symmetries of D to show that the bosonization of an atomic insulator state yields a ground state of the toric code (a deconfined \mathbb{Z}_2 gauge theory). The atomic insulator state $|\psi_{AI}\rangle$ is the unique ground state of the Hamiltonian: $H_{AI} = -\sum_f P_f$. H_{AI} is certainly unfrustrated, so $|\psi_{AI}\rangle$ satisfies $P_f |\psi_{AI}\rangle = |\psi_{AI}\rangle$ for all f . Applying D to $|\psi_{AI}\rangle$, we find:

$$D|\psi_{AI}\rangle = D \cdot P_f |\psi_{AI}\rangle = W_f \cdot D|\psi_{AI}\rangle, \forall f. \quad (51)$$

Therefore, the bosonized state $D|\psi_{AI}\rangle$ is in the $+1$ eigenspace of W_f for all f . Given the constraint on the image of D , the bosonized state is also in the $+1$ eigenspace of G_v for all v . Hence, $D|\psi_{AI}\rangle$ is a ground state of the unfrustrated Hamiltonian $H = -\sum_v G_v - \sum_f W_f$. Recalling the definition of G_v defined in Eq. (32):

$$G_v = \prod_{e \supset v} X_e \prod_{f: f_0=v} W_f, \quad (52)$$

we see that the G_v terms in H can be replaced by $\prod_{e \supset v} X_e$ without changing the ground states. ($G_v = \prod_{e \supset v} X_e$ in the subspace where $W_f = 1$.) Thus, $D|\psi_{AI}\rangle$ is a ground state of the toric code Hamiltonian $H_{TC} = -\sum_v \prod_{e \supset v} X_e - \sum_f W_f$.

To gain intuition for the mapping, we consider acting with D on a state with non-trivial fermion occupancy. In particular, we apply a hopping operator S_e at edge e to the atomic insulator state $|\psi_{AI}\rangle$ to obtain a state with fermions at the two faces neighboring e . The image of $S_e |\psi_{AI}\rangle$ under D is:

$$D \cdot S_e |\psi_{AI}\rangle = U_e \cdot D|\psi_{AI}\rangle = U_e |\psi_{TC}\rangle. \quad (53)$$

U_e (defined in Eq.(30)) creates a \mathbb{Z}_2 flux (-1 eigenvalue of W_f) at each face bordering the edge e and moves \mathbb{Z}_2 charges (-1 eigenvalue of $\prod_{e \supset v} X_e$) to the 0-vertices of L_e and R_e . A \mathbb{Z}_2 flux bound to a \mathbb{Z}_2 charge has fermionic statistics – it is an *emergent* fermion. Therefore, physical fermions are mapped to emergent fermions in the \mathbb{Z}_2 gauge theory. The gauge constraint $G_v = 1, \forall v$ removes ambiguity in this mapping, since it enforces that charges are bound to fluxes, with the charges located at the 0-vertex of the corresponding triangle.

Any fermion parity even state can be created from $|\psi_{AI}\rangle$ by applying operators in \mathcal{E} . Hence, one strategy for mapping an arbitrary even fermion parity state $|\psi_f\rangle$ is to identify an even operator $\mathcal{O}(\{S_e\}_e, \{P_f\}_f)$, written here explicitly in terms of the generators of \mathcal{E} , such that:

$$|\psi_f\rangle = \mathcal{O}(\{S_e\}_e, \{P_f\}_f) |\psi_{AI}\rangle. \quad (54)$$

Then, the duality maps:

$$|\psi_f\rangle \rightarrow \mathcal{O}(\{U_e\}_e, \{W_f\}_f) |\psi_{TC}\rangle. \quad (55)$$

In general, it may be challenging to find an operator, expressed in terms of the generators of \mathcal{E} , that creates $|\psi_f\rangle$ from $|\psi_{AI}\rangle$. Moreover, the analysis of bosonizing states, thus far, has only required the operator-level bosonization duality. In the next section, we illustrate the true potential of the bosonization TNO. Given a fermion parity even state $|\psi_f\rangle$ constructed from the contraction of local tensors, we show that $|\psi_f\rangle$ can be bosonized by using D to modify each of the local tensors. The resulting state can then be written as a bosonic tensor network state.

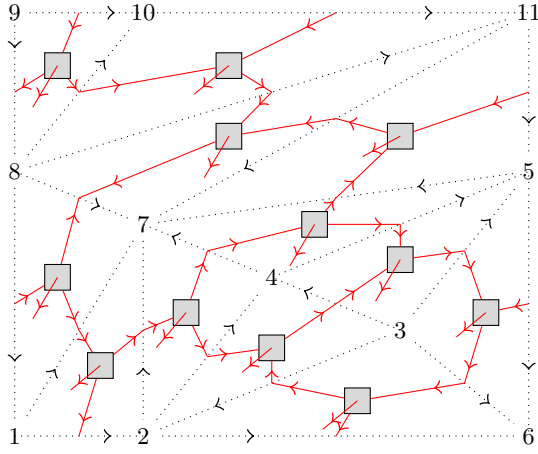


FIG. 4. An example fPEPS on an arbitrarily triangulated torus. The square nodes represent the tensors T and \bar{T} in Eqs. (56) and (57). The legs affixed to the center of the square nodes and pointing out of the page are the physical legs of the fPEPS. All other legs are contracted with a leg of a neighboring tensor.

IV. BOSONIZATION OF FPEPS

In the previous section, we introduced the bosonization of a fermionic state $|\psi_f\rangle$ as the action of the bosonization TNO D on $|\psi_f\rangle$. As we now show, the TNO is especially useful when the fermionic $|\psi_f\rangle$ is represented as a fermionic tensor network state. While the action of D on the fermionic tensor network state $|\psi_f\rangle$ indeed yields a bosonic state $D|\psi_f\rangle = |\psi_b\rangle$, $|\psi_b\rangle$ is not manifestly a bosonic tensor network state. This is due, in part, to the \mathbb{Z}_2 -graded virtual legs of the bosonization TNO. However, if $|\psi_f\rangle$ is in the form of a fermionic projected entangled pair state (fPEPS) (see Fig. 4 for an example), we can explicitly rewrite $|\psi_b\rangle$ as a bosonic projected entangled pair state (bPEPS). In this section, we give a detailed algorithm for converting bosonized fPEPS into bPEPS, which is well defined on arbitrary triangulations of orientable 2D manifolds without boundary.

A. Contracting the bosonization TNO with an fPEPS

An fPEPS on a triangulated manifold is built from \mathbb{Z}_2 -graded tensors $T[f']$ on positively oriented triangles and $\bar{T}[f']$ on negatively oriented triangles.

Assuming that the tensors are fermion parity even, they can be written in component form as:

$$\begin{aligned} T[f'] &\equiv \sum_{a,b,c} T_{abc}^{(f')} |c\rangle_{f'_{01}} |a\rangle_{f'_{12}} \langle b|_{f'_{02}} (a + b + c|_{f'} \\ \bar{T}[f'] &\equiv \sum_{a,b,c} \bar{T}_{abc}^{(f')} |b\rangle_{f'_{02}} \langle a|_{f'_{12}} |c\rangle_{f'_{01}} (a + b + c|_{f'}, \end{aligned} \quad (56)$$

where for generality, the tensor components are posi-

tion dependent. $T[f']$ and $\bar{T}[f']$ can then be represented, respectively, as follows:

$$\begin{aligned} &\begin{array}{c} f'_{02} \\ \downarrow \\ \text{[T]} \\ \uparrow \\ f'_{01} \end{array}, \begin{array}{c} f'_{01} \quad f'_{12} \\ \swarrow \quad \searrow \\ \text{[\bar{T}]} \\ \downarrow \\ f'_{02} \end{array} \quad (57) \end{aligned}$$

Fig. 4 shows an fPEPS formed from contracting $T[f']$ and $\bar{T}[f']$ on an arbitrary triangulation of a torus.

In general, one can insert matrix product operators (MPO) before closing an fPEPS on a closed manifold. Though we believe our construction can be extended to such cases, in the interest of brevity and clarity, we restrict the discussion to fPEPS without any MPO insertions.

To apply D to an fPEPS $|\psi_f\rangle$, we contract the physical indices of F tensors with those of the T tensors, and likewise, we contract \bar{F} tensors with \bar{T} tensors. Thus, the first step in bosonizing an fPEPS is to calculate the tensors $M_f = F \cdot T$ for positively oriented triangles and the tensors $\bar{M}_f = \bar{F} \cdot \bar{T}$ for negatively oriented triangles. Graphically, M_f and \bar{M}_f can be drawn, respectively, as:

$$\begin{aligned} &\begin{array}{c} f'_{02} \\ \downarrow \\ \text{[M}_f\text{]} \\ \uparrow \\ f'_{01} \end{array}, \begin{array}{c} f'_{01} \quad f'_{12} \\ \swarrow \quad \searrow \\ \text{[\bar{M}_f\text{]} \\ \downarrow \\ f'_{02} \end{array} \quad (58) \end{aligned}$$

The bosonized state $|\psi_b\rangle$ is a tensor network state (in fact an fPEPS) generated by tensors M_f , \bar{M}_f , as well as $B_\eta[e]$ on edges. Since there are two layers of virtual legs to be contracted, we refer to them as the “state layer” and the “TNO layer”. Note that M_f and \bar{M}_f tensors have virtual legs on both layers, but $B_\eta[e]$ is only on the TNO layer.

While $|\psi_b\rangle$ is a tensor network state and an fPEPS, it is not generically a bPEPS, as there are fermionic virtual indices remaining. The challenge is then to re-express $|\psi_b\rangle$ as a bPEPS, or, in a sense, to convert the fermionic virtual legs to bosonic virtual legs. We accomplish this by systematically accounting for the signs accrued in contracting the fermionic virtual legs – the so-called *Koszul signs*. To make our strategy clear, we first discuss Koszul signs and introduce the idea of a *removable grading*. These concepts play a key role in the rest of this section, so we describe them in generality before returning to the problem of converting the fermionic virtual legs of $|\psi_b\rangle$ to bosonic virtual legs.

B. Koszul signs and removable grading

The bosonized fPEPS encodes a bosonic quantum state $|\psi_b\rangle = \sum_{\{\phi\}} C_\phi |\phi\rangle$, where the collection of $|\phi\rangle$ form a complete set of product states. The coefficients C_ϕ can be

recovered from the bosonized fPEPS by fixing the physical indices according to $|\phi\rangle$ and summing over the virtual indices. Given the \mathbb{Z}_2 -grading of the virtual legs, there are signs picked up upon re-ordering and contracting the \mathbb{Z}_2 -graded vectors, which can contribute to the coefficient C_ϕ . A natural question is whether the grading of a virtual index is essential to the tensor network, i.e., if the grading of a particular virtual index is removed, does the value of the bosonized fPEPS change?

For illustration, consider the two simple graded tensors $A = \sum_{a,a'} A_{aa'}(a'|_s \langle a|_t$ and $B = \sum_{b,b'} B_{bb'}(b'|_s \langle b|_t$. (We can think of s and t as indices corresponding to the state and TNO layers, respectively.) We want to calculate the tensor network (which is a scalar in this case) $A \cdot B$. Let us describe the contraction of these tensors as a two step process. In the first step, we contract the basis tensors:

$$(a'|_s \langle a|_t \cdot |b'\rangle_s \langle b|_t) = (-1)^{|b'| |a|} \delta_{ab} \delta_{a'b'}, \quad (59)$$

and in the second step, we calculate the components:

$$\sum_{a,a,b,b'} (-1)^{|b'| |a|} \delta_{ab} \delta_{a'b'} A_{aa'} B_{bb'} = \sum_{a,a'} (-1)^{|a'| |a|} A_{aa'} B_{aa'}. \quad (60)$$

Notice that we produce an additional sign of $(-1)^{|b'| |a|}$ in the basis contraction step due to the graded nature of indices. This is the key difference between virtual indices of fermionic and bosonic tensor networks – bosonic indices do not produce any additional signs in basis contraction. We refer to these additional signs of basis contractions as Koszul signs. The point is that the grading of a virtual index contributes to the fPEPS only through possible Koszul signs. Therefore, we can remove the grading of a virtual index as long as we properly account for the Koszul signs.

Sometimes this can be done simply by picking a specific internal ordering for the fermionic tensors and interpreting their components, with respect to this ordering, as components of purely bosonic tensors. We say that the grading of the virtual indices in the original fermionic tensor network can be removed, if the contraction of this new bosonic tensor network is the same as that of the original fermionic tensor network. When we have some a priori internal ordering for the fermionic tensors in mind already – one that does produce Koszul signs – then we can refer to this process as *changing the internal ordering* to eliminate the Koszul signs. For example, consider changing the internal ordering of A to $A = \sum_{a,a'} A_{aa'} (-1)^{|a'| |a|} (a|_t \langle a'|_s$. Now, there is no Koszul sign in the basis contraction: $(a|_t \langle a'|_s \cdot |b'\rangle_s \langle b|_t) = \delta_{a,b} \delta_{a',b'}$. Removing the grading from A and B yields:

$$\begin{aligned} A_b &= \sum_{a,a'} A_{aa'} (-1)^{|a'| |a|} \langle a|_t \langle a'|_s \\ B_b &= \sum_{b,b'} B_{bb'} |b'\rangle_s |b\rangle_t. \end{aligned} \quad (61)$$

A_b and B_b are purely bosonic tensors, and they produce the same tensor network: $A_b \cdot B_b = A \cdot B$. Note that the grading is removable for only particular choices of the internal ordering.

In other cases, the Koszul signs can be accounted for with a removal of the grading, followed by an insertion of additional operators into the tensor network. To see an example of this, consider the two even tensors $A = \sum_a A_a |a\rangle_p \langle a|_q$ and $B = \sum_b B_b |b\rangle_q \langle b|_p$. We then aim to compute the tensor network (a scalar) $\text{tr}[A \cdot B]$, where the \cdot denotes the contraction of the q leg and the trace over the p index is to emphasize that we are contracting the first index with the last index to close the loop. Contracting the basis tensors yields:

$$\text{tr}[|a\rangle_p \langle a|_q \cdot |b\rangle_q \langle b|_p] = \delta_{ab} \text{tr}[|a\rangle_p \langle b|_p] = (-1)^{|a|} \delta_{ab}. \quad (62)$$

The grading of the q vector did not produce a sign, so it can be removed without affecting the tensor network. However, if we try to remove the grading of the p vector as well, the sign $(-1)^{|a|}$ is no longer accounted for. One way to reproduce the sign $(-1)^{|a|}$ is to insert a $Z = \sum_c (-1)^{|c|} |c\rangle \langle c|$ operator on leg p after removing the grading. That is, grading removal gives bosonic tensors $A_b = \sum_a A_a |a\rangle_p \langle a|_q$ and $B_b = \sum_b B_b |b\rangle_q \langle b|_p$, which satisfy:

$$\begin{aligned} \text{tr}[A_b \cdot B_b \cdot Z_p] &= \sum_{a,b,c} (-1)^{|c|} A_a B_b \text{tr}[|a\rangle_p \langle a|_q \cdot |b\rangle_q \langle b|_p \cdot |c\rangle_p \langle c|_p] \\ &= \text{tr}[A \cdot B] \end{aligned} \quad (63)$$

When the grading of a virtual index can be accounted for by inserting an additional operator O on un-graded indices, we will say that the grading is “removable with O -insertion”.

C. Koszul signs in the bosonized fPEPS

We now return to the problem of re-writing the bosonized fPEPS as an explicit bPEPS. We will find that, for a particular internal ordering, the grading of the virtual legs in the bosonized fPEPS is removable with $(Z_t \otimes Z_s)^{\eta_e}$ -insertion. Here, Z_t is a Pauli Z operator acting in the TNO layer, and Z_s is a Pauli Z operator acting in the state layer. In other words, the state represented by the bosonized fPEPS may be equivalently represented by the bPEPS obtained by removing the grading of the virtual legs (assuming a certain internal ordering) and applying $(Z_t \otimes Z_s)^{\eta_e}$ before contracting the tensors at each edge. To show this, we will compute the Koszul signs explicitly. We will see that the Koszul signs have a nice geometric interpretation in terms of the branching structure of the triangulated manifold.

1. Simplifying the Koszul sign calculation

We begin by simplifying the problem. First, $B_\eta = Z^{\eta_e} \cdot B$ does not contribute to any Koszul signs, since B_η

can always be contracted with one of its neighboring M_f or \bar{M}_f tensors without any change of internal ordering. This is possible due to the even parity of B_η and its simple, two-virtual-leg form $B_\eta = \sum_a (-1)^{a\eta_e} |a\rangle_e \langle a|_e$. Therefore, the Koszul signs accrued in contracting the tensors M_f , \bar{M}_f , and B_η are equivalent to the Koszul signs from directly contracting the M_f and \bar{M}_f tensors without B_η .

We continue to simplify the calculation of the Koszul signs by reducing M_f and \bar{M}_f from two layers of fermionic virtual legs as in Eq. (58) to a single layer of fermionic virtual legs. The first step is to choose the following internal ordering for the tensors M_f and \bar{M}_f , respectively:

$$(64)$$

Notice that for outward pointing legs (ket vectors), the state layer index comes before the TNO layer index, while for inward pointing legs (bra vectors), the order is reversed. Letting $|a\rangle_s$ and $|a\rangle_t$ be the state and TNO layer vectors, respectively, then with the ordering in Eq. (64), we have $\langle a|_t \langle a'|_s \cdot |a'\rangle_s |a\rangle_t = 1$, and no Koszul sign is produced between a' and a . Therefore, we can combine the legs and consider a composite index (a', a) with tensors written in terms of $|a', a\rangle_{st}$ and $\langle a', a|_{st}$. The Hilbert space of the composite leg corresponds to the Hilbert space of two spinless fermions. This is isomorphic to a single spinless fermion and a spin-1/2 under the isomorphism:

$$|a', a\rangle \leftrightarrow |a + a'\rangle |a\rangle. \quad (65)$$

Since the spin-1/2 degree of freedom does not affect the Koszul signs, we may disregard it for the present computation.

In summary, we have reduced the calculation of the Koszul signs of the bosonized fPEPS to a calculation of the Koszul signs obtained in the contraction of single layer tensors with internal orderings inherited from Eq. (64) and pictured below:

$$(66)$$

In Eq. (66), we have again used triangular nodes, but these tensors should not be confused with the four legged F and \bar{F} tensors. It should be noted that similar simplifications can be performed for the contraction (inner

product) of any two fPEPS (built from fermion parity even local tensors). Consequently, the calculation of the Koszul signs below holds more generally than the application at hand – turning a bosonized fPEPS into a bPEPS.

2. Contraction of basis tensors

As mentioned in section IV B, the contraction of tensors can be performed in two steps: (i) the basis tensors are contracted, and (ii) the components are calculated. The Koszul signs arise only in the first step. Therefore, to calculate the Koszul signs, we focus on the contraction of basis tensors with the ordering in Eq. (66). We denote the set of basis tensors at a positively oriented face f as $\mathcal{Q}[f]$ and the set of basis tensors at a negatively oriented face f as $\bar{\mathcal{Q}}[f]$. Explicitly, we have:

$$\begin{aligned} \mathcal{Q}[f] &= \{|a + b\rangle_{f_{01}} \langle a\rangle_{f_{12}} \langle b|_{f_{02}}, a, b = 0, 1\} \\ \bar{\mathcal{Q}}[f] &= \{|b\rangle_{f_{02}} \langle a|_{f_{12}} \langle a + b|_{f_{01}}, a, b = 0, 1\}. \end{aligned} \quad (67)$$

Note that the tensors in $\mathcal{Q}[f]$ and $\bar{\mathcal{Q}}[f]$ are fermion parity even by construction. M_f and \bar{M}_f are fermion parity even, so their component value for any fermion parity odd basis tensor is necessarily zero. Thus, we can disregard fermion parity odd basis tensors in computing the Koszul signs.

We now analyze the contraction of basis tensors in Eq. (67). For each triangle, we have an independently chosen element of either $\mathcal{Q}[f]$ or $\bar{\mathcal{Q}}[f]$ (depending on the orientation of f). The resulting product of basis tensors evaluates to 0, -1, or 1. If an odd vector $|1\rangle$ is paired with an even vector $|0\rangle$ at any edge, then the product is 0. (This is simply the statement that $\langle 0|1\rangle = \langle 1|0\rangle = 0$.) Thus, the configurations of basis tensors that evaluate to a nonzero value must have odd legs paired at edges. Since the elements of $\mathcal{Q}[f]$ and $\bar{\mathcal{Q}}[f]$ have even fermion parity (an even number of odd legs), this implies that the odd legs form closed loops (on the dual lattice) for any configuration that gives a nonzero value.

The computation of the Koszul signs then distills down to calculating the ± 1 valued contraction of configurations with closed loops of $|1\rangle$ states at edges. To formalize the problem, we define g_e as the $\{0, 1\}$ valued index at the edge e , and $\hat{\sigma}(\{g_e\}) = \pm 1$ as the sign obtained by evaluating the tensor contractions corresponding to the configuration $\{g_e\}$.

3. Basis contraction and cohomology

To make our arguments precise, we find it convenient to describe configurations of odd edges using the language of cohomology. To this end, we define a 0-cochain as a sum $\sum_v g_v \mathbf{v}$, where \mathbf{v} is a \mathbb{Z}_2 -valued function of vertices such that \mathbf{v} evaluates to 1 on the vertex v and 0 otherwise, and g_v are coefficients in \mathbb{Z}_2 . Similarly, 1-cochains and 2-cochains may be defined as

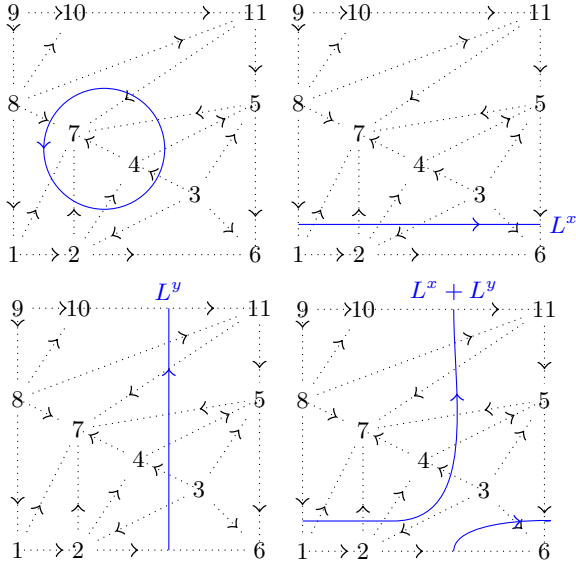


FIG. 5. Examples of 1-cochains. Edges intersected by the blue line have coefficient $g_e = 1$, while all other edges have $g_e = 0$. The top left picture is an example of a contractible 1-cocycle. The other three pictures are representative 1-cocycles of the three non-trivial classes.

sums $\sum_e g_e \mathbf{e}$ and $\sum_f g_f \mathbf{f}$, respectively. A configuration of odd edges $\{g_e\}$ then naturally corresponds to the 1-cochain $\sum_e g_e \mathbf{e}$. Furthermore, j -cochains can be added by combining the coefficients component wise, i.e., $\sum_e g_e \mathbf{e} + \sum_e g'_e \mathbf{e} = \sum_e (g_e + g'_e) \mathbf{e}$.

The *coboundary operator* δ from j -cochains to $j + 1$ -cochains is defined by:

$$\delta \mathbf{v} = \sum_{e \supset v} \mathbf{e}, \quad \delta \mathbf{e} = \sum_{f \supset e} \mathbf{f}, \quad (68)$$

where the sum on the left is over all edges sharing the vertex v and the sum on the right is over the two faces bordering the edge e . For example, in Fig. 5:

$$\begin{aligned} \delta \langle 4 \rangle &= \langle 2, 4 \rangle + \langle 3, 4 \rangle + \langle 4, 5 \rangle + \langle 4, 7 \rangle \\ \delta \langle 4, 7 \rangle &= \langle 2, 4, 7 \rangle + \langle 4, 5, 7 \rangle \end{aligned} \quad (69)$$

We call a cochain C *closed* if $\delta C = 0$. Note that each of the 1-cochains depicted in Fig. 5, for example, are closed. More generally, a closed 1-cochain, or 1-cocycle, can be thought of as a sum of loops along the dual lattice. As such, the configurations $\{g_e\}$, obtained from basis contraction, are examples of 1-cocycles.

A 1-cochain C is called a *1-coboundary* if there exists a 0-cochain R such that $C = \delta R$. δ can be understood as a boundary operator on the dual lattice, so intuitively, a 1-coboundary is a boundary of a region on the dual lattice. For example, the top left picture of Fig. 5 depicts a 1-coboundary – it is equal to δR for $R = \langle 7 \rangle + \langle 4 \rangle$. In general, 1-coboundaries are sums of contractible loops, which are generated by small loops $L_v \equiv \delta \mathbf{v}$ enclosing

a single vertex. A configuration L with a single, contractible loop is a 1-coboundary of a 0-cochain R containing vertices enclosed by the loop, i.e., $L = \sum_{v \in L} L_v$ with the sum being over vertices v enclosed by L . Some loops of odd edges such as the 1-cocycles L^x , L^y , and $L^x + L^y$ in Fig. 5, are *non-contractible*. These are 1-cocycles that cannot be written as δR for any 0-cochain R .

We can further define an equivalence of 1-cocycles where $C_1 \sim C_2$ if there exists a 0-cochain R such that $C_1 = C_2 + \delta R$. In other words, two 1-cocycles are equivalent if one can be constructed from the other by appending, or adding contractible loops. Hence, all 1-coboundaries belong to the same equivalence class – the class of trivial 1-cocycles. For a torus, it is well known that there are four inequivalent classes of 1-cocycles. These may be represented by L^x , L^y , $L^x + L^y$, and δR for a 0-cochain R . Therefore, an arbitrary 1-cocycle on a torus can be expressed as:

$$C = g_x L^x + g_y L^y + \sum_v g_v L_v, \quad (70)$$

for some choice of $g_x, g_y, g_v \in \mathbb{Z}_2$.

4. Koszul signs from a single loop

Given that a 1-cocycle can be decomposed in terms of constituent loops, as in Eq. (70), we begin by calculating the Koszul sign $\hat{\sigma}(L)$ for configurations L with a single loop of odd edges along the path L in the dual lattice. To propose an exact value for $\hat{\sigma}(L)$, we introduce the following notation. We assign a direction to the path L so that, with respect to a global orientation of the 2D manifold, the loop has a “left side” and a “right side”.²¹ L overlaps with a triangle f at two edges, and we call the common vertex of these two edges f_L . There are six possibilities for f_L : it can be a 0-, 1-, or 2-vertex of the triangle f , and it can lie to the left or to the right of the loop. We let \bar{l}_L and \bar{r}_L be the sets of f_L for which f_L is a 1-vertex of f and is to the left or right of L , respectively. We use $n(\bar{l}_L)$ and $n(\bar{r}_L)$ to denote the cardinality of \bar{l}_L and \bar{r}_L . Then we have:

Proposition 1.

$$\hat{\sigma}(L) = -(-1)^{\frac{1}{2}(n(\bar{l}_L) - n(\bar{r}_L))}. \quad (71)$$

Proof. See Appendix B. \square

5. Winding number and Koszul signs

$\hat{\sigma}(L)$ is closely related to the winding number of a certain vector field along the oriented path L . In particular, $\hat{\sigma}(L)$ can be computed from the continuous, non-vanishing vector field \mathcal{V} obtained from the branching structure by interpolating it into the interior of the triangles, as shown in Fig. 6 (see Ref. [22]). To calculate

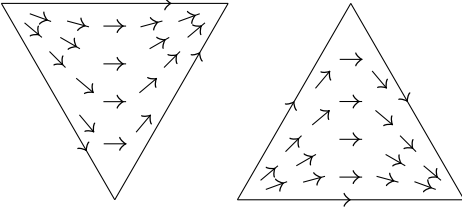


FIG. 6. The branching structure is interpolated into the interior of each triangle to form the continuous, non-vanishing vector field \mathcal{V} .

the winding number of \mathcal{V} along L we define \hat{n} to be the left pointing unit normal vector of the loop L and \hat{v} to be the local vector of \mathcal{V} . Then, we integrate the derivative of the angle $\theta = \cos^{-1}(\hat{v} \cdot \hat{n})$ between \hat{n} and \hat{v} along L . Given that θ is continuous, the change in θ around L must be $2\pi m$, where m is an integer. m gives the winding number of \mathcal{V} along L , which we denote as $w(L)$.²³ For definiteness, we choose clockwise rotation to be positive.

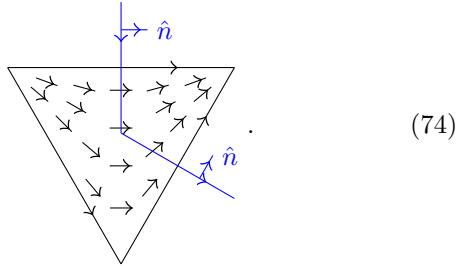
Proposition 2.

$$w(L) = \frac{1}{2}(n(\bar{l}_L) - n(\bar{r}_L)). \quad (72)$$

Equivalently,

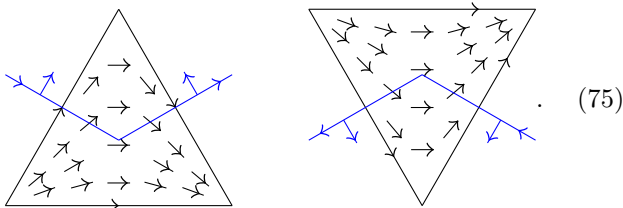
$$\hat{\sigma}(L) = -(-1)^{w(L)}. \quad (73)$$

Proof. We consider the ways in which L can pass through triangles and in each case, identify the change in $\theta = \cos^{-1}(\hat{v} \cdot \hat{n})$. When f_L is a 0- or 2-vertex, the total change in θ is 0. This is illustrated in the following example, where f_L is a 2-vertex:

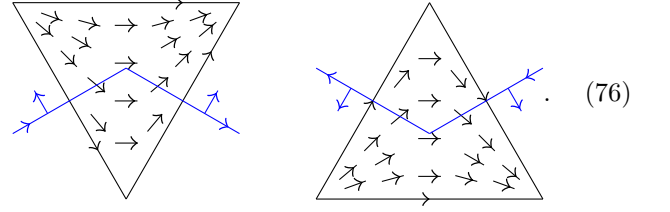


The change in θ through the triangle above is 0, since the vector field is nearly parallel to \hat{n} along the path. A similar argument applies whenever f_L is a 0- or 2-vertex. Thus, the only crossings that can contribute to the winding number are when f_L is a 1-vertex.

We first examine the case where f_L is a 1-vertex to the left of L , i.e., $f_L \in \bar{l}_L$. There are two such crossings:



(Note the triangle on the left is negatively oriented while the triangle on the right is positively oriented.) For both crossings, moving along L , the vector field rotates clockwise relative to \hat{n} , and θ changes by $+\pi$. If instead, f_L is to the right of L then the corresponding crossings are:



We see that, in this case, the vector field winds counter-clockwise along L , and θ changes by $-\pi$.

In conclusion, whenever f_L belongs to \bar{l}_L , θ changes by π , and when f_L is in \bar{r}_L , θ changes by $-\pi$. Accordingly, the winding number along L , with respect to \hat{n} , is:

$$w(L) = \sum_{f_L} \left(\frac{1}{2} \delta_{f_L \in \bar{l}_L} - \frac{1}{2} \delta_{f_L \in \bar{r}_L} \right) = \frac{1}{2}(n(\bar{l}_L) - n(\bar{r}_L)), \quad (77)$$

where $\delta_{f_L \in \bar{l}_L}$ and $\frac{1}{2} \delta_{f_L \in \bar{r}_L}$ are indicator functions for the sets \bar{l}_L and \bar{r}_L , respectively. \square

In Refs. [24,22], it is argued that a function on loops of the form $-(-1)^{w(L)}$, such as $\hat{\sigma}(L)$, gives a *quadratic refinement of the intersection pairing*. This is to say that, as a consequence of Prop. 2, $\hat{\sigma}$ satisfies:

$$\hat{\sigma}(L_1 + L_2) = (-1)^{\langle L_1, L_2 \rangle} \hat{\sigma}(L_1) \hat{\sigma}(L_2), \quad (78)$$

where $\langle L_1, L_2 \rangle$ is the intersection number (mod 2) of L_1 and L_2 . For example, the non-contractible cycles L^x and L^y on a torus in Fig. 5 have an intersection number $\langle L^x, L^y \rangle = 1 \bmod 2$. Therefore, by Eq. (78), we have: $\hat{\sigma}(L^x + L^y) = -\hat{\sigma}(L^x) \hat{\sigma}(L^y)$.

Importantly, Eq. (78) allows us to relate the sign $\hat{\sigma}(C)$ for a general configuration $C = \sum_i L_i$ to the signs $\hat{\sigma}(L_i)$ of constituent loops. For a single contractible loop L , which can be decomposed into a sum of loops $L = \sum_{v \in L} L_v$, the sign $\hat{\sigma}(L)$ can be written as [using Eq. (78)]:

$$\hat{\sigma}(L) = \prod_{v \in L} \hat{\sigma}(L_v). \quad (79)$$

The product in Eq. (79) is over vertices enclosed by the loop L .

We call a vertex v *singular* if the loop L_v , enclosing only v , is such that $\hat{\sigma}(L_v) = -1$. Referring to Eq. (79), the sign $\hat{\sigma}(L)$ for a contractible loop L can be computed by simply counting the singular vertices enclosed by L . Explicitly, $\hat{\sigma}(L)$ for a contractible loop L is:

$$\hat{\sigma}(L) = (-1)^{n_{sv}(L)}, \quad (80)$$

where $n_{sv}(L)$ is the number of singular vertices enclosed by the loop L . This is a manifestation of Stokes' theorem

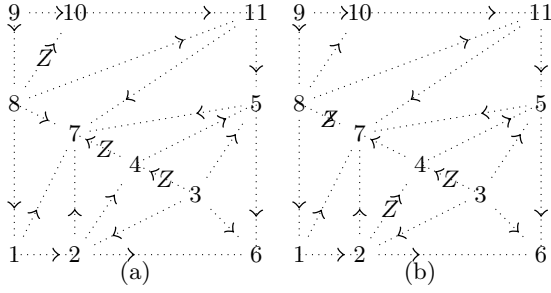


FIG. 7. An arbitrary triangulation of a torus with the four singular vertices: $\langle 3 \rangle$, $\langle 7 \rangle$, $\langle 5 = 8 \rangle$, $\langle 2 = 10 \rangle$, $\langle 2 = 11 \rangle$. (a) Z -operators placed at edges corresponding to the spin-structure $\eta = \{\langle 3, 4 \rangle, \langle 4, 7 \rangle, \langle 8, 10 \rangle\}$. (b) Z -operators placed at edges for an alternative choice of spin-structure $\eta = \{\langle 3, 4 \rangle, \langle 4, 2 \rangle, \langle 7, 8 \rangle\}$.

for the winding number of the vector field along L . We note that, using Prop. 1, a vertex v is singular if it is the 1-vertex of $4m$ triangles, for an integer m . Alternatively, using Prop. 2, v is singular if $-(-1)^{w(L_v)} = -1$.

D. Removing grading and choosing spin-structure

The function $\hat{\sigma}$ captures the Koszul signs accrued in the contraction of the fermionic virtual legs of the bosonized fPEPS. The goal of this section is to replace the \mathbb{Z}_2 -graded virtual legs of the bosonized fPEPS with un-graded legs and simulate the Koszul signs given by $\hat{\sigma}$ by inserting Pauli Z operators on certain bosonic virtual legs.

More specifically, we first convert the fermionic virtual legs to bosonic virtual legs, i.e., with the internal ordering fixed, we map a fermion parity even state $|0\rangle$ to an up spin $|0\rangle$ (in the Z basis) and a fermion parity odd state $|1\rangle$ to a down spin $|1\rangle$. The bosonic virtual legs fail to replicate the Koszul signs that were obtained by contracting the fermionic virtual legs. Thus, second, we fix this by choosing a set of edges η (a choice of spin-structure) and including an extra Z operator on edges $e \in \eta$ before contraction. When down spins $|1\rangle$ contract on an edge $e \in \eta$, the extra Pauli Z operator results in a sign -1 . We need to choose η so that the contraction of a configuration C of loops of down spins $|1\rangle$ yields the sign $\hat{\sigma}(C)$.

We begin by accounting for the Koszul signs $\hat{\sigma}(L)$ accrued by contractible loops L . Next, we discuss a matrix product operator (MPO) which captures the Koszul signs from non-contractible loops. We focus on the case when the manifold is a torus and only outline the procedure for more general 2D manifolds.

1. Reproducing Koszul signs for contractible loops

Our strategy for accounting for $\hat{\sigma}(L)$, when L is a contractible loop is to ‘pair-up’ the singular vertices and construct the set η from edges that connect the two singular vertices in each pair. More precisely, Stokes’ theorem guarantees an even number of singular vertices on a closed manifold, so we can always find a set of edges η such that the boundary of η gives the set of singular vertices. Here, the boundary of η is defined as the set of vertices that are endpoints of an odd number of edges in η . Intuitively, η can then be understood as ‘pairing-up’ singular vertices with each other through arbitrary paths. Fig. 7 provides an example of choosing η on a torus.

To replicate the sign $\hat{\sigma}(L)$, we insert Z operators on all edges in η (see Fig. 7). Now, in evaluating a configuration with a single loop L of down spins $|1\rangle$, we incur the sign:

$$\sigma_\eta(L) \equiv (-1)^{n(L,\eta)}, \quad (81)$$

where $n(L,\eta)$ denotes the number of common edges (or crossings) between the loop L and the edges in η . Given our construction of η , $n(L,\eta)$ is equal (mod 2) to the number of singular vertices enclosed in L . Therefore, for any contractible loop L :

$$\sigma_\eta(L) = (-1)^{n_{sv}(L)}, \quad (82)$$

in agreement with Eq. (80). Consequently, for any 1-cycle C and 0-cochain R , we have:

$$\sigma_\eta(C + \delta R) = \sigma_\eta(C) \sigma_\eta(\delta R) = \sigma_\eta(C) \prod_{v \in R} \sigma_\eta(L_v). \quad (83)$$

The product $\prod_{v \in R}$ is over all vertices such that the coefficient of \mathbf{v} in R is nontrivial.

We note that a choice of η can be modified by including any set of edges forming a contractible loop. We call two sets η and η' equivalent spin-structures, if one can be obtained from the other by appending contractible loops of edges.

2. Reproducing Koszul signs for non-contractible loops

$\sigma_\eta(C)$ simulates $\hat{\sigma}(C)$ for trivial 1-cocycles C . This is sufficient to account for Koszul signs when the fermionic system is defined on a sphere or an infinite plane. However, $\sigma_\eta(C)$ does not capture the sign $\hat{\sigma}(C)$ when C is a non-trivial 1-cocycle. To account for the Koszul signs on a torus or higher genus manifolds, we insert MPOs along non-contractible loops to perform a certain sum over inequivalent spin-structures. In the following, we describe the case of a torus in detail and only sketch the generalization to higher genus manifolds.

To start, we consider a particular triangulation of a torus without any singular vertices, as shown in Fig. 8(a-c). Since there are no singular vertices, $\hat{\sigma}(L) = 1$ for any contractible loop L . For non-contractible loops, however,

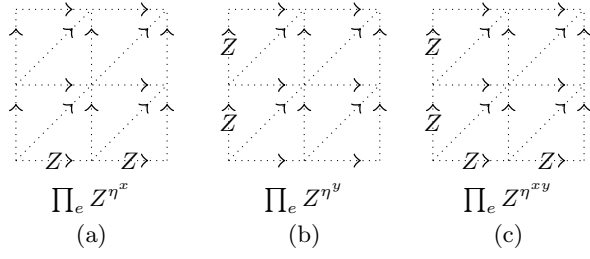


FIG. 8. Triangulation of a torus without any singular vertices, but with Z -operators placed along (a) the x -axis (b) the y -axis (c) both the x -axis and the y -axis.

the Koszul signs are non-trivial. To see this, we let L^x and L^y be distinct non-contractible loops lying parallel to the x -axis and y -axis, respectively. The specific choices of L^x and L^y do not matter, because contractible loops can freely be appended without changing $\hat{\sigma}(L^x)$ and $\hat{\sigma}(L^y)$. This follows from Eq. (78) and the fact that there are no singular vertices. Now, using either Prop. 1 or Prop. 2, one finds:

$$\hat{\sigma}(L^x) = \hat{\sigma}(L^y) = \hat{\sigma}(L^x + L^y) = -1. \quad (84)$$

Hence, after converting the \mathbb{Z}_2 -graded virtual legs to bosonic virtual legs, a modification is necessary to simulate the sign in Eq. (84). A possible solution is to insert Pauli Z operators along non-contractible loops. Naively, we can insert Z operators along only the x -axis [Fig. 8(a)], only the y -axis [Fig. 8(b)], or both the x -axis and the y -axis [Fig. 8(c)]. We find that all of these options fail to reproduce the sign in Eq. (84). The solution is a certain superposition of these options, which can be expressed using an MPO. Before describing this MPO, we develop some notation and discuss the effects of inserting Z operators along the axes.

First, we define the spin-structure η^x , which contains the edges along the x -axis. The product of Z operators applied along the edges in η^x can be expressed as $\prod_e Z_e^{\eta^x}$, where, in this expression, η^x is the indicator function for the set η^x . The operator $\prod_e Z_e^{\eta^x}$ is pictured in Fig. 8(a). Then, letting $\sigma_{\eta^x}(L)$ be the sign obtained in contracting a configuration of down spins along L with the added operator $\prod_e Z_e^{\eta^x}$, we have:

$$\sigma_{\eta^x}(L^x) = 1, \quad \sigma_{\eta^x}(L^y) = -1, \quad \sigma_{\eta^x}(L^x + L^y) = -1. \quad (85)$$

Next, we define the spin-structures η^y and η^{xy} similarly. η^y is the set of edges along the y -axis and corresponds to the insertion of the operator $\prod_e Z_e^{\eta^y}$, depicted in Fig. 8(b). In this case, the sign accrued in contracting the bosonic legs is:

$$\sigma_{\eta^y}(L^x) = -1, \quad \sigma_{\eta^y}(L^y) = 1, \quad \sigma_{\eta^y}(L^x + L^y) = -1. \quad (86)$$

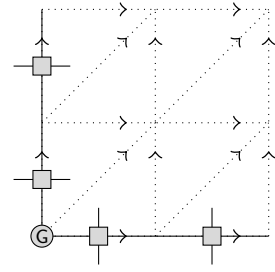


FIG. 9. Triangulation of a torus without any singular vertices, and with the MPOs generated by W (square nodes) and G (circular nodes). The MPOs generated by W wrap around both the x -axis and the y -axis and the G tensor is placed at their intersection.

If we instead insert Z operators along both the x -axis and y -axis, as in Fig. 8(c), and define η^{xy} as the union of η^x and η^y , we obtain the signs:

$$\sigma_{\eta^{xy}}(L^x) = -1, \quad \sigma_{\eta^{xy}}(L^y) = -1, \quad \sigma_{\eta^{xy}}(L^x + L^y) = 1. \quad (87)$$

In each case above [Eqs. (85)-(87)], the operator insertion fails to replicate the sign in Eq. (84). However, the sign in Eq. (84) can be simulated using the following superposition of operators:

$$\frac{1}{2} \left(-1 + \prod_e Z_e^{\eta^x} + \prod_e Z_e^{\eta^y} + \prod_e Z_e^{\eta^{xy}} \right). \quad (88)$$

Explicitly, the sign obtained in contracting an arbitrary loop of down spins L is then:

$$\frac{1}{2} (-1 + \sigma_{\eta^x}(L) + \sigma_{\eta^y}(L) + \sigma_{\eta^{xy}}(L)). \quad (89)$$

One can check that, for loops L^x , L^y , and $L^x + L^y$, the sign given by Eq. (89) matches the sign in Eq. (84). Furthermore, the sign in Eq. (89) agrees with $\hat{\sigma}$ on all loops.

The operator in Eq. (88) can be represented using MPOs. We start by considering an MPO of the form:

$$\dots \text{---} \boxed{W} \text{---} \boxed{W} \text{---} \boxed{W} \text{---} \dots, \quad (90)$$

generated by the local tensors W , given by:

$$\begin{aligned} \begin{array}{c} s \\ | \\ p \text{---} \boxed{W} \text{---} q \\ | \\ r \end{array} &= \sum_{a,b} (-1)^{(a)(b)} |a\rangle_p |b\rangle_r \langle b|_s \langle a|_q \\ &= |0\rangle I \langle 0| + |1\rangle Z \langle 1|. \end{aligned} \quad (91)$$

When the virtual (horizontal) legs take value 0, W acts as the identity, and when they take value 1, W acts as a Z operator. Therefore, W generates a controlled Z operator of the form $\dots III \dots + \dots ZZZ \dots$

If we insert this MPO on the virtual level of the bosonic tensor network, say, along the x -axis, it is equivalent to inserting the operator $1 + \prod_e Z_e^{\eta^x}$. Similarly, inserting it along the y -axis is equal to the operator $1 + \prod_e Z_e^{\eta^y}$. If we insert the MPO along both the x -axis and the y -axis they cross as a single vertex, and we link the MPOs together at their intersection using another tensor \mathbf{G} (see Fig. 9). We take \mathbf{G} to be:

$$\begin{aligned} \begin{array}{c} s \\ | \\ \textcircled{\mathbf{G}} \\ | \\ r \end{array} \begin{array}{c} p \\ \text{---} \\ q \end{array} &= \frac{1}{2} \sum_{a,b} (-1)^{(a+1)(b+1)} |a\rangle_p |b\rangle_r \langle b|_s \langle a|_q \\ &= -\frac{1}{2} |0\rangle_p |0\rangle_r \langle 0|_s \langle 0|_q + \frac{1}{2} |0\rangle_p |1\rangle_r \langle 1|_s \langle 0|_q \\ &\quad + \frac{1}{2} |1\rangle_p |0\rangle_r \langle 0|_s \langle 1|_q + \frac{1}{2} |1\rangle_p |1\rangle_r \langle 1|_s \langle 1|_q. \end{aligned} \quad (92)$$

Now, when virtual legs of the MPOs in both the x and y direction take value 0, \mathbf{G} is $-\frac{1}{2}$, and otherwise it is $\frac{1}{2}$. Thus, the total MPO produces the superposition of operators:

$$\frac{1}{2} \left(-1 + \prod_e Z_e^{\eta^x} + \prod_e Z_e^{\eta^y} + \prod_e Z_e^{\eta^x} \prod_e Z_e^{\eta^y} \right). \quad (93)$$

Recalling that η^{xy} is the union of η^x and η^y , we see that the operator above is equivalent to the operator in Eq. (88). The Koszul signs, therefore, can be accounted for using the MPO generated by \mathbf{W} and \mathbf{G} , pictured in Fig. 9.

In effect, the MPO implements a sum over inequivalent spin-structures to capture the Koszul signs of non-contractible loops. The tensor \mathbf{G} dictates the particular sum over spin-structures and, in general, depends on the branching structure. To see this, we next consider a general triangulation of a torus, where we must incorporate σ_η , accounting for singular vertices, with the sum over inequivalent spin-structures given by the MPO.

3. General triangulation of a torus

Thus far, we have argued that we can account for Koszul signs in the following two cases: (i) trivial 1-cocycles formed from contractible loops of $|1\rangle$ states and (ii) non-contractible loops formed by $|1\rangle$ states in the absence of singular vertices. To reproduce the Koszul signs from contraction on a general triangulation of a torus, we then must be able to simulate the Koszul signs from non-contractible loops in the presence of singular vertices. We will find that we require a branching structure dependent choice of the tensor \mathbf{G} to obtain an appropriate sum over inequivalent spin-structures.

The first step is to account for the Koszul signs of contractible loops, as in IV D 1. That is, we choose a set

of edges η such that the edges in η pair up the singular vertices and insert Z operators at the edges in η . The sign from evaluating a loop L of down spins is then $\sigma_\eta(L)$ as in Eqs. (81) and (82).

After choosing η we can account for the Koszul signs from non-contractible loops. As before, we choose representative non-contractible loops L^x and L^y lying parallel to the x - and y -axis, respectively, such as those in Fig. 5. However, unlike the case with no singular vertices, the choice of L^x and L^y matters. For example, the sign $\hat{\sigma}(L^x)$ changes if L^x is shifted across a singular vertex. Likewise the sign of $\sigma_\eta(L^x)$ changes if L^x is shifted across a singular vertex. Therefore, to remove the ambiguity, we define the $\{0, 1\}$ valued α_x and α_y by:

$$(-1)^{\alpha_x} \equiv \hat{\sigma}(L^x) / \sigma_\eta(L^x) \quad (94)$$

$$(-1)^{\alpha_y} \equiv \hat{\sigma}(L^y) / \sigma_\eta(L^y) \quad (95)$$

$$(-1)^{\alpha_x + \alpha_y + 1} = \hat{\sigma}(L^x + L^y) / \sigma_\eta(L^x + L^y). \quad (96)$$

We emphasize that the expressions above are independent of the particular choice of representative non-contractible loops L^x and L^y , using Eqs. (78) and (83).

We now only need to reproduce the signs on the left side of Eqs. (94), (95), and (96) for non-contractible loops using the MPO generated by \mathbf{W} and \mathbf{G} . A superposition of operators that yields these signs from contracting bosonic legs is:

$$\begin{aligned} \frac{1}{2} (-1)^{\alpha_x \alpha_y} &\left(1 + (-1)^{\alpha_y} \prod_e Z_e^{\eta^x} \right. \\ &\quad \left. + (-1)^{\alpha_x} \prod_e Z_e^{\eta^y} + (-1)^{\alpha_x + \alpha_y} \prod_e Z_e^{\eta^{xy}} \right). \end{aligned} \quad (97)$$

It can be shown that this operator is generated by \mathbf{W} and \mathbf{G} with the components of \mathbf{G} given by:

$$G_{ab} = \frac{1}{2} (-1)^{(\alpha_y + a)(\alpha_x + b)}. \quad (98)$$

For the special case of the triangulation in Fig. 8, $\alpha_x = \alpha_y = 1$ and Eq. (98) gives $G_{ab} = \frac{1}{2} (-1)^{(a+1)(b+1)}$, which matches our previous result. Given the spin structure in Fig. 12, $\alpha_x = \alpha_y = 0$. Thus, in this case, to capture the Koszul signs from non-contractible loops, the components of \mathbf{G} should be $G_{ab} = \frac{1}{2} (-1)^{ab}$.

4. Higher genus manifolds

We briefly describe how our results can be extended to higher genus manifolds. We exploit the fact that any 2D oriented manifold M with genus g is topologically equivalent to a manifold constructed from the connected sum $\#$ of a sphere with g torii: $M \simeq S^2 \# T^2 \# \dots \# T^2$. Furthermore, given a decomposition of M into a connected sum of a sphere and torii, any cocycle C can be written

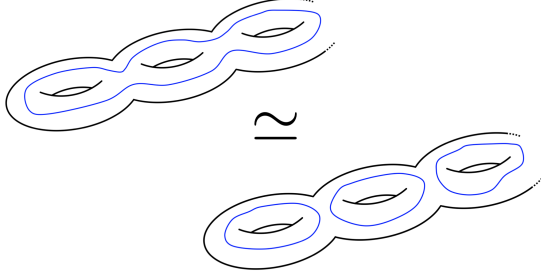


FIG. 10. A cocycle on a genus g manifold is cohomologous to a \mathbb{Z}_2 sum of cocycles on the component tori. The non-trivial cocycles on independent tori on the right hand side have a trivial intersection number.

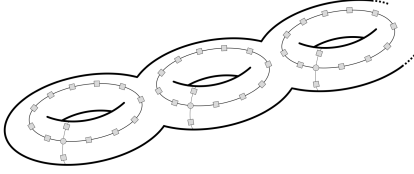


FIG. 11. MPOs generated by W and G are inserted on each component tori. The G tensor may differ between the tori.

as:

$$C = \sum_{j=1}^g a_{j,x} L^{j,x} + \sum_{j=1}^g a_{j,y} L^{j,y} + \delta R. \quad (99)$$

Here, $L^{j,x}$ and $L^{j,y}$ denote generators of the non-trivial cocycles around the j^{th} torus in the connected sum decomposition, and δR gives a trivial cocycle. According to Eq. (99), any cocycle C is cohomologous to one of the form [see Fig. 10]:

$$\sum_{j=1}^g a_{j,x} L^{j,x} + \sum_{j=1}^g a_{j,y} L^{j,y}. \quad (100)$$

With this, we can now describe how to account for the Koszul signs from contraction on a genus g manifold. As before, the Koszul signs from contractible loops can be taken care of by making a choice of η and inserting Pauli Z operators along the edges in η . As for non-trivial cocycles, we first decompose the cocycle as in Eq. (99). Then, we identify the cohomologous cocycle given in Eq. (100), which differs by a trivial cocycle. (The difference in the Koszul sign between the cohomologous cocycles is already accounted for by the choice of η .) Using that the Koszul sign corresponds to a quadratic refinement of the intersection pairing [Eq. (78)], the computation of the Koszul signs for a cocycle in the form of Eq. (100) reduces to a computation of the Koszul signs for the loops $L^{j,x}$ and

$L^{j,y}$. This is because loops belonging to different tori have trivial intersection number:

$$\langle L^{x,j}, L^{x,k} \rangle = \langle L^{x,j}, L^{x,k} \rangle = \langle L^{x,j}, L^{x,k} \rangle = 0 \mod 2, \quad (101)$$

for all $j \neq k$. Therefore, the problem is reduced to that of g independent arbitrarily triangulated tori. The Koszul signs of non-contractible loops can be accounted for by inserting MPOs generated by W and G as in Fig. 11. A similar strategy as in section IV D 3 can be used to choose G at each intersection of the MPOs.

5. Grading removal for the bosonized fPEPS

Now, we return to the original problem of writing bosonized fPEPS as bPEPS. To compute the Koszul signs, we worked with a single layer of fermionic virtual legs, while a bosonized fPEPS has both the state layer and TNO layer of fermionic virtual legs. Therefore, we need to translate our results for accounting for Koszul signs back to the case of two layers of virtual legs.

To simplify the calculation of the Koszul sign, we noticed that [Eq.(65)], with the chosen ordering of the fermionic virtual legs, the pair of virtual legs $|a\rangle_t |a'\rangle_s$ could be mapped to a spinless fermionic degree of freedom and a spin-1/2 via the isomorphism:

$$|a\rangle_t |a'\rangle_s \rightarrow |a + a'\rangle |a\rangle. \quad (102)$$

Then, we worked only with the fermionic leg. Ultimately, we converted the fermionic legs $|a + a'\rangle$ to bosonic legs $|a + a'\rangle$ with the addition of Z operators on certain edges. A Z operator acting on $|a + a'\rangle$ corresponds to acting with a parity operator on $|a + a'\rangle$ or the operator $P_s \otimes P_t$ on $|a\rangle_t |a'\rangle_s$. Therefore, to replace the two layers of fermionic legs with two layers of bosonic legs: $|a\rangle_t |a'\rangle_s \rightarrow |a\rangle_t |a'\rangle_s$, we see that we need to apply operators $Z_t \otimes Z_s$ at edges to account for Koszul signs.

In summary, we convert the two layers of fermionic legs (with the fixed internal ordering) to bosonic legs. Then, we insert $(Z_t \otimes Z_s)^{\eta_e}$ at every edge to account for the Koszul signs from contractible loops. To account for the Koszul signs from non-contractible loops, we modify the MPO so that W in Eq. (91) is: $|0\rangle(I_t \otimes I_s)|0\rangle + |1\rangle(Z_t \otimes Z_s)|1\rangle$.

E. Algorithm for bosonizing an fPEPS

The following gives an algorithm for bosonizing an fPEPS on a torus and writing it explicitly as a bPEPS.

1. Given a triangulated 2D manifold with branching structure, determine the singular vertices. Singular vertices are those that are 1-vertices of $4m$ number of triangles. Pair singular vertices along convenient paths. The edges along these paths are the elements of η .

V. CONCLUSION AND FUTURE WORK

Tensor networks provide a powerful framework for studying quantum many-body systems. Their simple parameterization allows for efficient numerical computations, and their diagrammatic representation elucidates the structure of entanglement in quantum states. More abstractly, tensor networks provide a uniform language for discussing quantum many-body systems. Here, we have extended the formalism of tensor networks to exact bosonization dualities. In particular, we have constructed a TNO that implements the two dimensional bosonization duality first discussed in Ref. [2]. Furthermore, our bosonization TNO can be applied directly to fermionic tensor network states, thus defining bosonization at the level of quantum states.

A critical step of our bosonization procedure is to express the bosonized state as an explicit bosonic tensor network. To this end, we described how to account for Koszul signs accrued in contracting fermionic tensor networks, and we constructed matrix product operators to be placed along non-trivial cycles for this purpose. As a result, our bosonization duality at the level of states can be applied to fermionic systems on arbitrary triangulations of 2D manifolds without a boundary.

We would also like to emphasize that the calculation of Koszul signs in section IV has potential for applications outside of the bosonization of fPEPS. In fact, the calculation applies to the contraction of *any*²⁵ 2D fPEPS generated by fermion parity even local tensors and without fermionic physical legs. In particular, it may be useful for efficiently evaluating the overlap between two fPEPS. Explicitly, one can use the technology developed in section IV to replace the fermionic virtual legs with bosonic virtual legs and account for the Koszul signs. Notably, for a regular triangular lattice or square lattice, our results show that the fermionic virtual legs can freely be replaced with bosonic virtual legs as long as the MPO generated by W and G is inserted before closing the tensor network on a manifold with non-trivial genus.

Directions for future work include generalizing our bosonization duality, identifying tensor network representations of wider classes of dualities, and utilizing the bosonization TNO to study fermionic systems. A natural generalization is to develop a 3D bosonization duality at the level of quantum states. Recently, [26] presented a bosonization duality in 3D, and we expect that this duality admits a tensor network representation. Formulating a TNO for the 3D duality might also make it clear how to bosonize in dimensions greater than three. Another possible generalization is to extend our bosonization duality to manifolds with boundaries.

It would be interesting to construct tensor network representations for other operator-level dualities. Ref. [19] describes a duality for parafermionization in 2D, in which a system of constrained spins is dual to a system of parafermions. Formulating a corresponding TNO would require a careful understanding of paraspin-structure –

a generalization of spin-structure to parafermions. We also expect that recently developed dualities for gauging subsystem symmetries can be naturally formulated in terms of tensor networks [27]. Further, it would be nice to interpret the results of Ref. [28] using tensor networks.

We anticipate that our bosonization procedure will be useful for studying fermionic topological orders. Beginning with a fermionic tensor network state, one can apply the bosonization procedure outlined in the text and subsequently analyze the topological order of the bosonic state using the myriad of techniques developed to study bosonic topological orders. In addition, MPO symmetries of the fermionic state can be tracked through the bosonization procedure to obtain the MPO symmetries of the bosonic system.

Going the other direction, the Hermitian conjugate of the bosonization TNO can be applied to a bosonic state to obtain a fermionic tensor network state. Two dimensional (non-chiral) bosonic topological orders have been well studied using tensor networks, so we can use the known tensor network representations of fixed point states to construct fixed point states for fermionic topological phases. Furthermore, the MPO symmetries of the bosonic system descend to MPO symmetries of the fermionic system. While fixed point states for intrinsic fermionic topological orders and fermionic symmetry protected topological phases were identified in Refs. [17,18], our bosonization procedure gives a means for constructing and studying fixed point states for fermionic symmetry-enriched topological orders as well.

Acknowledgements – SS would like to acknowledge Alex Turzillo for valuable discussions about related work on \mathbb{Z}_2 -graded tensors. SS and TE also thank Dave Aasen for helpful conversations about fermion condensation. LF is supported by NSF DMR-1519579.

Appendix A: \mathbb{Z}_2 -graded tensor representation of Majorana operators

In this appendix, we show that the tensors introduced in section II and rewritten here:

$$e \leftarrow \gamma \leftarrow e = \sum_a |a+1\rangle_e \langle a|_e \quad (A1)$$

$$e \leftarrow \hat{\gamma} \leftarrow e = \sum_a (-1)^a |a+1\rangle_e \langle a|_e, \quad (A2)$$

are indeed good representations of Majorana operators. To do so, we explicitly show that the algebraic relations of the Majorana tensors match those of the Majorana operators introduced in section IID.

We begin by analyzing the algebra at a single site e . To this end, we apply the Majorana tensors to an arbitrary state A at site e :

$$e \leftarrow A \equiv \sum_a A_a |a\rangle_e.$$

According to section IID, at site e , $\gamma_e^2 = \bar{\gamma}_e^2 = 1$. Applying a single γ tensor to \mathbf{A} , we find:

$$\begin{aligned} e \leftarrow \gamma \leftarrow \mathbf{A} &\equiv \sum_b |b+1\rangle_e (b|_e^c \sum_a A_a |a\rangle_e^c) \quad (\text{A3}) \\ &= \sum_a A_a |a+1\rangle_e. \end{aligned}$$

Then, acting with another γ on $\gamma\mathbf{A}$ gives:

$$\begin{aligned} e \leftarrow \gamma \leftarrow \gamma \leftarrow \mathbf{A} &\equiv \sum_b |b+1\rangle_e (b|_e^c \sum_a A_a |a+1\rangle_e^c) \quad (\text{A4}) \\ &= \sum_a A_a |a\rangle_e. \end{aligned}$$

Since \mathbf{A} was arbitrary, we see that γ contracted in succession with another γ acts as the identity. The relation $\bar{\gamma}_e^2 = 1$, can be shown similarly.

Next, we show that the relation $\bar{\gamma}_e \gamma_e = -\gamma_e \bar{\gamma}_e$ is represented by the Majorana tensors. $\bar{\gamma}\gamma\mathbf{A}$ is:

$$\begin{aligned} e \leftarrow \bar{\gamma} \leftarrow \gamma \leftarrow \mathbf{A} &\equiv \sum_c (-1)^c i |c+1\rangle_e (c|_e^{c_2} \sum_b |b+1\rangle_e^{c_2} (b|_e^{c_1} \sum_a A_a |a\rangle_e^{c_1}) \\ &= - \sum_a (-1)^a i |a\rangle_e, \quad (\text{A5}) \end{aligned}$$

while $\gamma\bar{\gamma}\mathbf{A}$ is:

$$\begin{aligned} e \leftarrow \gamma \leftarrow \bar{\gamma} \leftarrow \mathbf{A} &\equiv \sum_b |b+1\rangle_e (b|_e^{c_2} \sum_c (-1)^c i |c+1\rangle_e^{c_2} (c|_e^{c_1} \sum_a A_a |a\rangle_e^{c_1}) \\ &= \sum_a (-1)^a i |a\rangle_e. \quad (\text{A6}) \end{aligned}$$

Comparing (A5) and (A6), we see that the tensors γ and $\bar{\gamma}$ capture the relation $\gamma_e \bar{\gamma}_e = -\bar{\gamma}_e \gamma_e$. It is important to note that in going from (A5) to (A6), the contractions are different. The difference in sign is not simply due to the odd grading of γ and $\bar{\gamma}$.

Now, we consider the algebraic relations of Majorana operators at different sites. Majorana operators acting at different sites anti-commute, so we must show that switching the order of contraction, for Majorana tensors applied to different legs yields a sign. This property follows from the odd grading of the Majorana tensors. We write an arbitrary state $|\psi\rangle$ with N two dimensional fermionic site Hilbert spaces as:

$$\begin{aligned} &\begin{array}{c} \uparrow \quad \uparrow \quad \dots \quad \uparrow \quad \uparrow \\ \boxed{|\psi\rangle} \end{array} \\ &= \sum_{a_1, \dots, a_N} \Psi_{a_1, \dots, a_N} |a_1\rangle_{e^1} \dots |a_N\rangle_{e^N}. \quad (\text{A7}) \end{aligned}$$

First acting with γ at site e^j and second acting with γ at site e^i , we have:

$$\begin{aligned} &\begin{array}{c} \uparrow \quad \gamma_i \quad \dots \quad \gamma_j \quad \uparrow \\ \boxed{|\psi\rangle} \end{array} \\ &\equiv \left(\sum_c |c+1\rangle_{e^i} (c|_{e^i}^{c_2} \right) \left(\sum_b |b+1\rangle_{e^j} (b|_{e^j}^{c_1} \right) \sum_{a_1, \dots, a_N} \Psi_{a_1, \dots, a_N} |a_1\rangle_{e^1} \dots |a_i\rangle_{e^i}^{c_1} \dots |a_j\rangle_{e^j}^{c_2} \dots |a_N\rangle_{e^N} \quad (\text{A8}) \end{aligned}$$

$$= \sum_{a_1, \dots, a_N} \Psi'_{a_1, \dots, a_N} |a_1\rangle_{e^1} \dots \left(\sum_c |c+1\rangle_{e^i} (c|_{e^i}^{c_2} \right) |a_i\rangle_{e^i}^{c_2} \dots \left(\sum_b |b+1\rangle_{e^j} (b|_{e^j}^{c_1} \right) |a_j\rangle_{e^j}^{c_1} \dots |a_N\rangle_{e^N} \quad (\text{A9})$$

$$= \sum_{a_1, \dots, a_N} \Psi'_{a_1, \dots, a_N} |a_1\rangle_{e^1} \dots \left(\sum_c |c+1\rangle_{e^i} (c|_{e^i}^{c_1} \right) |a_i\rangle_{e^i}^{c_1} \dots \left(\sum_b |b+1\rangle_{e^j} (b|_{e^j}^{c_2} \right) |a_j\rangle_{e^j}^{c_2} \dots |a_N\rangle_{e^N} \quad (\text{A10})$$

$$= \left(\sum_c |c+1\rangle_{e^i} (c|_{e^i}^{c_1} \right) \left(\sum_b |b+1\rangle_{e^j} (b|_{e^j}^{c_2} \right) \sum_{a_1, \dots, a_N} \Psi_{a_1, \dots, a_N} |a_1\rangle_{e^1} \dots |a_i\rangle_{e^i}^{c_1} \dots |a_j\rangle_{e^j}^{c_2} \dots |a_N\rangle_{e^N} \quad (\text{A11})$$

$$= - \left(\sum_b |b+1\rangle_{e^j} (b|_{e^j}^{c_2} \right) \left(\sum_c |c+1\rangle_{e^i} (c|_{e^i}^{c_1} \right) \sum_{a_1, \dots, a_N} \Psi_{a_1, \dots, a_N} |a_1\rangle_{e^1} \dots |a_i\rangle_{e^i}^{c_1} \dots |a_j\rangle_{e^j}^{c_2} \dots |a_N\rangle_{e^N} \quad (\text{A12})$$

$$= - \begin{array}{c} \uparrow \quad \uparrow \quad \uparrow \quad \uparrow \\ \textcircled{\gamma_i} \quad 1 \quad \dots \quad \textcircled{\gamma_j} \quad 2 \\ \hline |\psi\rangle \end{array} \quad (\text{A13})$$

In (A9), we have absorbed the signs from moving the Majorana tensors past odd vectors into the coefficient Ψ' . After moving the Majorana tensors, the ordering of the contractions are switched [line (A10)]. Lastly, we have moved the Majorana tensors to the left and interchanged their order [(A11) and (A12)]. The contraction \mathcal{C}_1 is then to the right of \mathcal{C}_2 , and we can read line (A12) as first a γ acts on site e^i then a γ acts on site e^j . We thus have that γ tensors acting on different sites anti-commute. Looking at (A8) and (A12), we see that the difference in sign is purely a consequence of the odd parity of γ . Indeed, more generally, γ tensors acting on different legs of an arbitrary tensor will anti-commute. An analogous calculation for $\bar{\gamma}$ tensors or a mixture of γ and $\bar{\gamma}$ tensors shows that they anti-commute when acting on different legs.

Appendix B: Calculation of the Koszul sign for a single loop

Here, we provide a proof of Prop. 1. We choose an arbitrary edge of the loop L to be e^0 and label the j^{th} edge of the path as e^j . Starting with the triangle following e^0 , along the orientation of L , we denote the j^{th} triangle on the path as f^j . For each triangle f^j , we have a specific basis tensor $Q_{f^j}^L$ from the set $\mathcal{Q}[f]$ or $\bar{\mathcal{Q}}[f]$ [see Eq. (67)] depending on the orientation of f^j . The sign to be calculated is then:

$$\hat{\sigma}(L) = \text{tr} [Q_{f^0}^L \cdot Q_{f^1}^L \cdot \dots \cdot Q_{f^n}^L]. \quad (\text{B1})$$

As already mentioned, there are six possible ways for the loop to cross a triangle. We list the six possible crossings of a positive triangle and its associated basis tensors $Q_{f^j}^L$ (ignoring legs with even parity):

$$\begin{aligned} \begin{array}{c} \uparrow \\ \textcircled{\gamma} \\ \uparrow \end{array} &\equiv |1\rangle_{e^j} |1\rangle_{e^{j+1}} = -i |1\rangle_{e^j} [i |1\rangle_{e^{j+1}}], \\ \begin{array}{c} \uparrow \\ \textcircled{\gamma} \\ \downarrow \end{array} &\equiv - |1\rangle_{e^j} |1\rangle_{e^{j+1}} = i |1\rangle_{e^j} [i |1\rangle_{e^{j+1}}], \\ \begin{array}{c} \downarrow \\ \textcircled{\gamma} \\ \downarrow \end{array} &\equiv |1\rangle_{e^{j+1}} |1\rangle_{e^j} = [i |1\rangle_{e^j}] [i |1\rangle_{e^{j+1}}], \end{aligned}$$

$$\begin{aligned} \begin{array}{c} \uparrow \\ \textcircled{\gamma} \\ \uparrow \end{array} &\equiv |1\rangle_{e^j} (1|_{e^{j+1}} \\ \begin{array}{c} \uparrow \\ \textcircled{\gamma} \\ \downarrow \end{array} &\equiv |1\rangle_{e^{j+1}} (1|_{e^j} = [i(1|_{e^j})] [i |1\rangle_{e^{j+1}}] \\ \begin{array}{c} \downarrow \\ \textcircled{\gamma} \\ \downarrow \end{array} &\equiv |1\rangle_{e^j} (1|_{e^{j+1}}. \end{aligned} \quad (\text{B2})$$

The blue arrows denote the loop L , which enters at edge e^j and exists from edge e^{j+1} . Notice that when the loop goes around a 0-vertex or a 2-vertex (bottom four pictures), both edges point to the same side of L , but when the loop goes around a 1-vertex (top two pictures), a right-left transition of edge directions occurs. The relation between the diagrams and the tensors can be summarized as follows:

- (i) Edges e^j pointing to the *right* of L contribute $(1|_{e^j}$ to the tensor $Q_{f^{j-1}}^L$ and $|1\rangle_{e^j}$ to the tensor $Q_{f^j}^L$.
- (ii) Edges e^j pointing to the *left* of L contribute $i |1\rangle_{e^j}$ to the tensor $Q_{f^{j-1}}^L$ and $i(1|_{e^j}$ to the tensor $Q_{f^j}^L$.
- (iii) If f_L is an 1-vertex, then we accrue an additional phase $i^{\delta_{f_L \in \bar{l}_L}} i^{-\delta_{f_L \in \bar{r}_L}}$, where $\delta_{f_L \in \bar{l}_L} = 1$ if $f_L \in \bar{l}_L$ and $\delta_{f_L \in \bar{r}_L} = 0$ otherwise. $\delta_{f_L \in \bar{r}_L}$ is defined similarly. Therefore, if f_L is a 1-vertex, we accrue a phase i , if it lies to the left of L or a phase $-i$, if it lies to the right of L .

Negatively oriented triangles also have 6 possible crossings. It can be checked that the same rules as in (i)-(iii) above apply to negative triangles. For example, consider the following crossing on a negative triangle:

$$\begin{array}{c} \uparrow \\ \textcircled{\gamma} \\ \downarrow \end{array} \equiv (1|_{e^{j+1}} (1|_{e^j}, \quad (\text{B3})$$

where the RHS is an element of (67) (ignoring even parity legs). Now, we verify that the rules (i)-(iii) yield the RHS

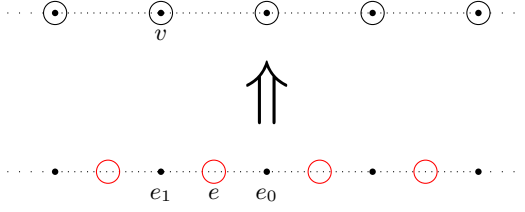


FIG. 13. The bosonization duality is a map from a fermionic system to a bosonic system. In the fermionic system there is a spinless complex fermion degree of freedom (red circles) at each edge e . In the bosonic system there is a spin-1/2 at each vertex v .

of Eq. (B3). Rule (ii) implies e^j contributes $i(1|_{e^j}$, rule (i) implies edge e^{j+1} contributes $(1|_{e^{j+1}}$, and finally, rule (iii) implies that the f_L vertex contributes an i phase. Putting it together, we get the tensor $i(1|_{e^j}(1|_{e^{j+1}}i = (1|_{e^{j+1}}(1|_{e^j}$, which is indeed the RHS of Eq. (B3). The other five cases of crossing across negatively oriented triangles can be checked similarly.

With this, we calculate the sign in Eq. (B1). We consider the contraction of tensors $Q_{f^{j-1}}^L$ and $Q_{f^j}^L$ at the edge e^j . If e^j points to the right of L , then, according to rule (i), $Q_{f^{j-1}}^L$ has $(1|_{e^j}$ and $Q_{f^j}^L$ has $(1|_{e^j}$. No Koszul sign is produced in contraction at e^j because $(1|_{e^j} \cdot 1|_{e^j} = 1$. Similarly, if e^j points to the left of L , then, according to rule (ii), $Q_{f^{j-1}}^L$ has $i(1|_{e^j}$ and $Q_{f^j}^L$ has $i(1|_{e^j}$, and again no Koszul sign is produced: $i(1|_{e^j} \cdot i(1|_{e^j} = 1$. The remaining sources of signs are triangles that contribute a sign $i^{\delta_{f_L \in \bar{L}}} i^{-\delta_{f_L \in \bar{r}_L}}$ according to rule (iii), and the overall -1 supertrace sign that comes from contracting the first and last indices in Eq. (B1). Therefore, the total sign is:

$$\begin{aligned} \hat{\sigma}(L) &= - \prod_{f_L} i^{\delta_{f_L \in \bar{L}}} i^{-\delta_{f_L \in \bar{r}_L}} \\ &= - i^{(n(\bar{L}) - n(\bar{r}_L))} = -(-1)^{\frac{1}{2}(n(\bar{L}) - n(\bar{r}_L))}. \end{aligned} \quad (\text{B4})$$

Note that $\hat{\sigma}(C)$ is always ± 1 , because the total number of transition points $n(\bar{L}) + n(\bar{r}_L)$ has to be even. This implies $n(\bar{L}) - n(\bar{r}_L)$ is even as well.

Appendix C: Tensor Network Bosonization in 1D

For completeness, we give a detailed description of the TNO representation of bosonization in 1D. To start, we present 1D bosonization as a map of local fermionic operators to local bosonic operators.

1. Review of 1D bosonization

On the fermionic side of the duality, we consider a one dimensional lattice with a spinless complex fermion at each edge, as pictured in Fig. 13. The complex fermion

at edge e may be described using the familiar fermionic creation and annihilation operators: c_e^\dagger, c_e . These generate the full fermionic operator algebra at e . However, it will be convenient to instead work with Majorana operators, $\gamma_e, \bar{\gamma}_e$, as discussed in section IID.

To ensure the bosonization duality maps local operators to local operators, we define the duality on a subset of the full fermionic operator algebra - the subalgebra of fermion parity even operators \mathcal{E} . The fermion parity even operators are those that commute with the global fermion parity operator $\prod_e P_e$, where P_e is the fermion parity at the edge e . \mathcal{E} can be generated by two types of operators: fermion parity P_e at each edge and the hopping operators S_v at each vertex v . The hopping operators transfer fermion parity between edges and are defined by:

$$S_v \equiv i\gamma_{L_v} \bar{\gamma}_{R_v}, \quad (\text{C1})$$

with L_v and R_v the edge to the left and right of vertex v , respectively. The hopping operators are mutually commuting and commute with all parity operators besides the neighboring two, i.e.:

$$S_v P_e = (-1)^{\delta_{v \subset e}} P_e S_v, \quad (\text{C2})$$

where $\delta_{v \subset e} = 1$ if vertex v is at one of the endpoints of the edge e and $\delta_{v \subset e} = 0$ otherwise. With open boundary conditions, the set of fermion parity operators and hopping operators are independent. However on a closed manifold they satisfy the relation:

$$\prod_v S_v \prod_e P_e = -1 \quad (\text{C3})$$

On the bosonic side of the duality we have a spin-1/2 at each vertex (see Fig. 13). The operator algebra of the spin-1/2 at vertex v can be generated by the Pauli operators: X_v, Z_v . Thus, the set of X_v and Z_v for all vertices generates the full bosonic operator algebra, which we denote as \mathcal{A} .

We now define the duality map $\mathfrak{D} : \mathcal{E} \rightarrow \mathcal{A}$ on the generators of \mathcal{E} :

$$\begin{aligned} \mathfrak{D}(P_e) &= Z_{e_0} Z_{e_1} \\ \mathfrak{D}(S_v) &= X_v. \end{aligned} \quad (\text{C4})$$

where e_0 and e_1 denote the vertices at the endpoints of e such that e points from e_0 to e_1 (Fig. 13). \mathfrak{D} is an injective homomorphism from \mathcal{E} to \mathcal{A} so that for $A_1, A_2 \in \mathcal{E}$:

$$\begin{aligned} \mathfrak{D}(A_1 + A_2) &= \mathfrak{D}(A_1) + \mathfrak{D}(A_2) \\ \mathfrak{D}(A_1 A_2) &= \mathfrak{D}(A_1) \mathfrak{D}(A_2). \end{aligned} \quad (\text{C5})$$

One can check that \mathfrak{D} preserves the commutation relations in (C2).

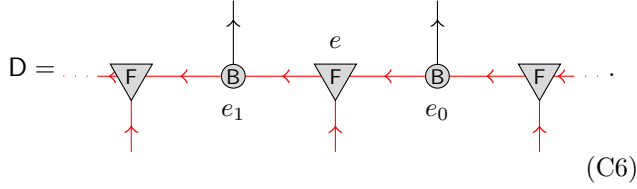
Note that the bosonization duality in Eq. (C4) is not the usual Jordan-Wigner transformation, defined, for example, in Ref. [29]. \mathfrak{D} is instead the composition of the familiar Jordan-Wigner transformation (restricted to

\mathcal{E}) with the Kramers-Wannier duality. We have chosen the duality \mathfrak{D} to define bosonization, because it is locality preserving and more naturally relates to the 2D bosonization in section III.

To translate the operator duality defined in (C4) to a TNO, we employ the formalism of \mathbb{Z}_2 -graded Hilbert spaces and graded tensor products.

2. TNO representation of the duality

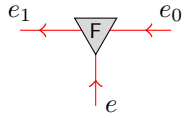
We now give a tensor network operator (TNO) representation D of the bosonization duality \mathfrak{D} in Eq. (C4). We begin with the following TNO ansatz:



$$D = \dots \text{F} \text{B} \text{F} \text{B} \text{F} \dots \quad (\text{C6})$$

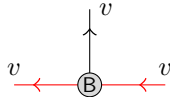
For now, we leave the boundary conditions of D unspecified – they will enter the construction later.

D is constructed by gluing together two kinds of local tensors, F (triangular nodes) and B (circular nodes), as pictured in (C6). An F tensor is placed at each edge e and is represented as follows:



$$\equiv \sum_{j,a,b} F_{a,b}^j |a\rangle_{e_1} \langle j|_e \langle b|_{e_0}. \quad (\text{C7})$$

At each vertex v , we place a tensor B :



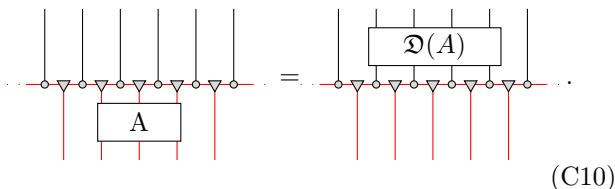
$$\equiv \sum_{j,a,b} B_{a,b}^j |a\rangle_v \langle j|_v \langle b|_v. \quad (\text{C8})$$

Notice that in Eq. (C7), we have three distinct Hilbert spaces labeled by the same site – one fermionic space (to which $|a\rangle_v$ belongs), one dual fermionic space (to which $\langle a|_v$ belongs) and one bosonic space (to which $|j\rangle_v$ belongs).

To implement the duality map \mathfrak{D} of Eq. (C4), we need to choose tensors F and B such that the following relations hold for all even operators $A \in \mathcal{E}$:

$$D \cdot A = \mathfrak{D}(A) \cdot D, \quad (\text{C9})$$

or diagrammatically:



$$(\text{C10})$$

Note that, we need only show that the relations are satisfied for P_e and S_v – the generators of \mathcal{E} . That is, we need to show that:

$$D \cdot P_e = \mathfrak{D}(P_e) \cdot D = Z_{e_0} Z_{e_1} \cdot D \quad (\text{C11a})$$

$$D \cdot S_v = \mathfrak{D}(S_v) \cdot D = X_v \cdot D. \quad (\text{C11b})$$

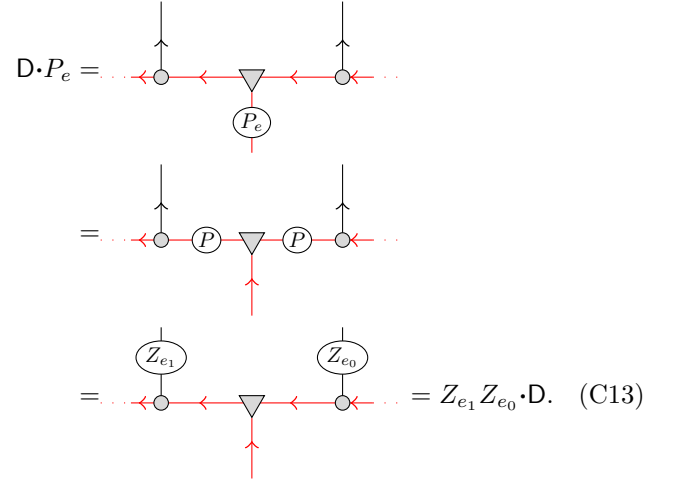
We can look at these constraints as symmetries of the tensor D , which can be reduced to symmetries of local tensors F and B . We claim that D satisfies (C11a) and (C11b) if F and B have the following symmetries:

$$F = P_{e_1} \cdot F \cdot P_{e_0} \cdot P_e = F \cdot i\gamma_e \cdot \bar{\gamma}_{e_0} = \bar{\gamma}_{e_1} \cdot F \cdot \bar{\gamma}_e \quad (\text{C12a})$$

$$B = P_v \cdot B \cdot P_v = Z_v \cdot B \cdot P_v = \bar{\gamma}_v \cdot X_v \cdot B. \quad (\text{C12b})$$

These symmetries are represented graphically in Fig. 14.

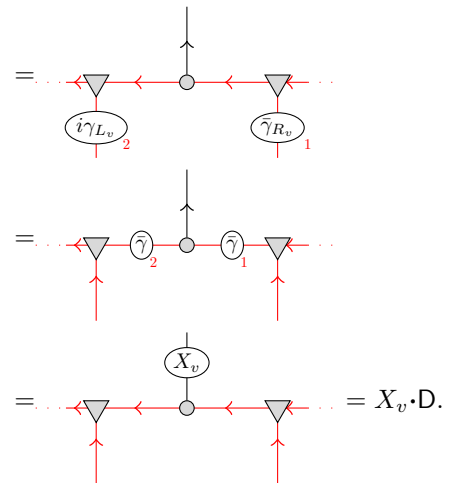
Using the diagrammatic representation of the symmetries, we can illustrate that D obeys (C11a) and (C11b). By successive applications of the symmetries in Fig. 14, we have:



$$D \cdot P_e = \dots \text{F} \text{B} \text{F} \text{B} \text{F} \dots \quad (\text{C13})$$

Similarly, for the hopping operator, we have:

$$D \cdot S_v = D \cdot i\gamma_{L_v} \bar{\gamma}_{R_v} \quad (\text{C14})$$



$$= \dots \text{F} \text{B} \text{F} \text{B} \text{F} \dots = X_v \cdot D.$$

Hence, D is a good representation of the operator duality \mathfrak{D} .

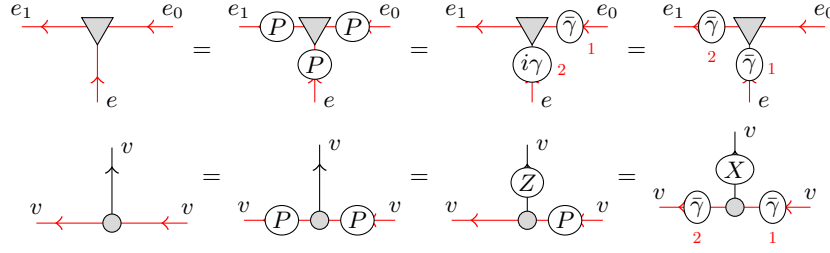


FIG. 14. Diagrammatic representation of the symmetries of F (first line) and B (second line) written algebraically in Eqs. (C12a) and (C12b).

Furthermore, we can use the symmetries of F and B to compute their explicit component form. Notice that the three symmetries of F are independent, commute with each other, and square to the identity. Thus, they generate a $\mathbb{Z}_2^3 = \mathbb{Z}_2 \times \mathbb{Z}_2 \times \mathbb{Z}_2$ symmetry group. Similarly, the three symmetries of B form a \mathbb{Z}_2^3 group. Since both tensors are vectors in a $2^3 = 8$ dimensional Hilbert space, the symmetries fix the tensors completely (up to a normalization). The explicit tensors can then be calculated by projecting the vacuum tensor onto the symmetric subspace:

$$F \propto \sum_{a,b,c} (\bar{\gamma}_{e_1} \bar{\gamma}_e)^a (i\gamma_e)^b P_{e_1}^c |0\rangle_{e_1} \langle 0|_e (0|_{e_0} P_e^c P_{e_0}^c \gamma_{e_0}^b = \sum_{a,b} |a\rangle_{e_1} (a+b|_e |b\rangle_{e_0}. \quad (C15)$$

Applying the same strategy to compute B , we find:

$$B \propto \sum_a |a\rangle_v |a\rangle_v \langle a|_v. \quad (C16)$$

Thus far, we have constructed a TNO that implements a map of local operators to local operators. In the next subsection, we will illustrate one of the key advantages of the TNO representation of the bosonization duality. That is, we will see that D may be applied to fermionic tensor network states to map them to bosonic tensor network states.

Appendix D: Bosonization of fermionic matrix product states

We now show that certain fermionic matrix product states (fMPS) can be directly bosonized using the bosonization TNO, D , defined in the previous subsection. In particular, we will describe the bosonization procedure for fMPS of the form:

$$|\psi\rangle = \left[\begin{array}{c} \uparrow \\ \text{---} \text{T} \text{---} \end{array} \right] \left[\begin{array}{c} \uparrow \\ \text{---} \text{T} \text{---} \end{array} \right] \left[\begin{array}{c} \uparrow \\ \text{---} \text{T} \text{---} \end{array} \right] \cdots \left[\begin{array}{c} \uparrow \\ \text{---} \text{T} \text{---} \end{array} \right] O_\psi \quad (D1)$$

where T is a fermion parity even tensor and O_ψ is an operator with definite parity. O_ψ is inserted before closing

the fermionic matrix product state to dictate the parity of the state and the boundary conditions. We will use vertical dash-dotted lines to denote closing the boundary (or taking the trace, algebraically). Unless otherwise stated, we assume the Hilbert spaces are two dimensional. Algebraically, $|\psi\rangle$ can be written as:

$$|\psi\rangle = \sum_{j_0, \dots, j_N} \text{tr} [T^{j_0} T^{j_1} \dots T^{j_N} O_\psi] |j_0\rangle_{e_0} |j_1\rangle_{e_1} \dots |j_N\rangle_{e_N}, \quad (D2)$$

where e^k denotes the edge connecting the $k-1$ vertex and the k vertex. The first step in bosonizing $|\psi\rangle$ is to close D with an operator O_D :

$$\left[\begin{array}{c} \uparrow \\ \text{---} \text{T} \text{---} \end{array} \right] \left[\begin{array}{c} \uparrow \\ \text{---} \text{T} \text{---} \end{array} \right] \cdots \left[\begin{array}{c} \uparrow \\ \text{---} \text{T} \text{---} \end{array} \right] O_D \quad (D3)$$

As we will show now, the choice of O_D determines both the subspace of the fermionic Hilbert space mapped non-trivially by the duality as well as the subspace of the bosonic Hilbert space in the image of the duality.

1. Boundary conditions in 1D

Here, we discuss how the choice of O_D affects the duality. With O_D parameterized as $O_D = (-i\bar{\gamma})^\alpha P^\beta$ and $\alpha, \beta \in \{0, 1\}$, we will show that α determines the parity of the fermionic states that are mapped to non-trivial bosonic states and β dictates the image of the duality. Specifically, for $\alpha = 0(1)$, the subspace of states with even (odd) parity are mapped to the subspace of bosonic states invariant under the operator $(-1)^{\beta+1} \prod_v X_v$.

To begin, we note that the choice of O_D does not affect the duality away from the boundary. Away from the boundary, the graphical calculation in (C13) and (C14) is unchanged by the choice of O_D . For a chain with $N+1$ sites, we constrain O_D by considering the image of the fermion parity operator P_{e_0} and the hopping operator S_N . (Recall that we have defined e^k as the edge connecting vertices $k-1$ and k , so e^0 connects 0 and N .) We will also require that, similar to the case away from the

boundary, D maps local operators near the boundary to local operators.

Now, we consider acting on P_{e^0} with D . The diagrammatic calculation yields:

$$\begin{aligned}
 D \cdot P &= \text{Diagram (D4)} \\
 &= \text{Diagram (D5)} \\
 &= Z_N Z_0 \cdot D'.
 \end{aligned}
 \tag{D4}$$

Note that the operator Z_N is required to ensure that the commutation relations between P_{e^0} and S_N are preserved by the duality. In the last line of (D4), D' is the same as D but with O_D replaced by $P O_D P$. The bosonization TNO should be left unmodified, so we require that $D' \propto D$. This means that $P O_D P = c O_D$ for some $c \in \mathbb{C}$, and we have:

$$D = D \cdot P_{e^0}^2 = c^2 D. \tag{D5}$$

Therefore, c must be ± 1 , or $P O_D P = \pm O_D$. We then see that O_D must have definite fermion parity, so it can be parameterized as $O_D = (-i\bar{\gamma})^\alpha P^\beta$ with $\alpha, \beta \in \{0, 1\}$.

Next, we act on the hopping operator S_N with D :

$$\begin{aligned}
 D \cdot S_N &= D \cdot i\gamma_{e^N} \bar{\gamma}_{e^0} \\
 &= (-1)^{|O_D|} \text{Diagram (D6)} \\
 &= (-1)^{|O_D|} X_N \cdot D''.
 \end{aligned}
 \tag{D6}$$

The factor of $(-1)^{|O_D|}$ is a consequence of moving $i\gamma_{e^N}$ past O_D . In the last line of (D6), D'' is the same as D except with O_D replaced by $\bar{\gamma} O_D \bar{\gamma}$. To obtain a relation as in (C9), we require that $D'' \propto D$. Assuming $\bar{\gamma} O_D \bar{\gamma} = a O_D$ for $a \in \mathbb{C}$, we obtain:

$$D = D \cdot S_N^2 = a^2 D, \tag{D7}$$

and thus, $a = \pm 1$.

We are now able to discuss the affect of O_D on the mapping of states. We define $D_{\alpha\beta}$ to be the TNO formed by closing D with O_D parameterized by $O_D = (-i\bar{\gamma})^\alpha (P)^\beta$. Then, (D4) and (D6) are summarized by:

$$D_{\alpha\beta} \cdot P_{e^0} = (-1)^\alpha Z_N Z_0 \cdot D_{\alpha\beta} \tag{D8}$$

$$D_{\alpha\beta} \cdot S_N = (-1)^{\alpha+\beta} X_N \cdot D_{\alpha\beta}. \tag{D9}$$

Acting on global fermion parity with $D_{\alpha\beta}$, we find:

$$\begin{aligned}
 D_{\alpha\beta} \cdot \prod_e P_e &= (-1)^\alpha \left(\prod_e Z_{e^0} Z_{e^1} \right) \cdot D_{\alpha\beta} \\
 &= (-1)^\alpha D_{\alpha\beta}.
 \end{aligned}
 \tag{D10}$$

This implies that $D_{\alpha\beta}$ maps fermionic states $|\psi\rangle$ with $|\psi| \neq \alpha$ to zero. Explicitly, we have:

$$\begin{aligned}
 D_{\alpha\beta} |\psi\rangle &= (-1)^{|\psi|} D_{\alpha\beta} \cdot \prod_e P_e |\psi\rangle \\
 &= (-1)^{|\psi|+\alpha} D_{\alpha\beta} |\psi\rangle.
 \end{aligned}
 \tag{D11}$$

Therefore, $D_{\alpha\beta} |\psi\rangle = 0$ whenever $|\psi| \neq \alpha$. To bosonize an even state, α should be equal to 0, and accordingly, O_D is proportional to I or P . For an odd state, one should use $\alpha = 1$, in which case, O_D is proportional to $-i\bar{\gamma}$ or γ .

To understand the role of the β parameter, we act on $D_{\alpha\beta}$ with $\prod_v X_v$:

$$\prod_v X_v \cdot D_{\alpha\beta} = (-1)^{\alpha+\beta} D_{\alpha\beta} \cdot \prod_v S_v. \tag{D12}$$

Now we use a global relation of the fermionic operator algebra. It can be checked that:

$$\prod_v S_v = - \prod_e P_e. \tag{D13}$$

Hence, continuing the calculation from (D12):

$$\begin{aligned}
 \prod_v X_v \cdot D_{\alpha\beta} &= (-1)^{\alpha+\beta+1} D_{\alpha\beta} \cdot \prod_e P_e \\
 &= (-1)^{\beta+1} D_{\alpha\beta}.
 \end{aligned}
 \tag{D14}$$

This means that the duality maps a fermionic state $|\psi\rangle$ to the $(-1)^{\beta+1}$ eigenspace of $\prod_v X_v$, as can be seen from the following:

$$\prod_v X_v \cdot D_{\alpha\beta} |\psi\rangle = (-1)^{\beta+1} D_{\alpha\beta} |\psi\rangle. \tag{D15}$$

We have thus shown that O_D can be parameterized by $O_D = (-i\bar{\gamma})^\alpha P^\beta$ with $\alpha, \beta \in \{0, 1\}$, and that D closed with O_D gives a map from the $(-1)^\alpha$ eigenspace of $\prod_e P_e$ to the $(-1)^{\beta+1}$ eigenspace of $\prod_v X_v$.

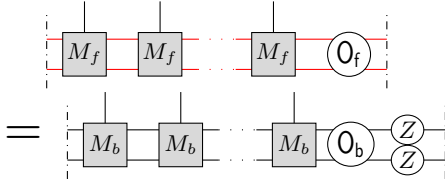
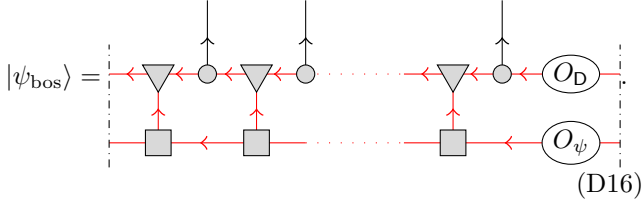


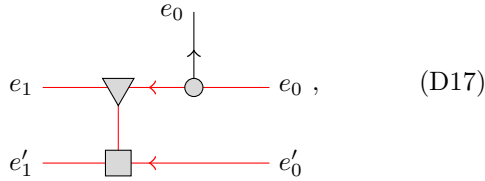
FIG. 15. With the internal ordering chosen in (D20) and (D22), the virtual legs of M_f and O_f can be replaced with ungraded virtual legs. The supertrace sign produced between the first and last indices on both layers is accounted for by inserting the operator $Z_N \otimes Z_{N'}$ before closing the state generated by M_b and O_b .

2. Converting virtual indices to bosonic indices

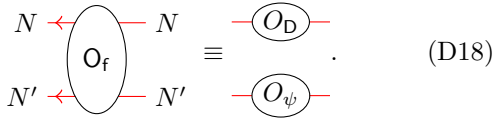
The second step is to contract D with $|\psi\rangle$ to form $|\psi_{\text{bos}}\rangle$:



We can then see that $|\psi_{\text{bos}}\rangle$ is built from the local tensors $M_f \equiv T \cdot F \cdot B$:



and the tensor network is closed with the operator $O_f \equiv O_\psi O_D$:

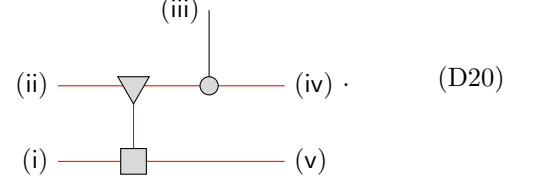


The state $|\psi_{\text{bos}}\rangle$ formed by contracting together M_f and closing with O_f is indeed a bosonic state. However, it is not manifestly a bosonic matrix product state (bMPS), since the virtual legs may have nontrivial grading.

In the third and final step of the bosonization procedure, we write $|\psi_{\text{bos}}\rangle$ as a bonafide bMPS – constructed from a local tensor with bosonic virtual legs. As suggested in section IV B, we do so by choosing a particular internal ordering of the virtual legs of M_f and O_f , in which they become convertible to bosonic indices. We start by writing M_f and O_f in tensor component form. In tensor component form, a generic M_f is:

$$M_f = \sum_{\substack{j, a', a, = 0 \\ b, b'}} (M_f)_{aa', b'b}^j |a'\rangle_{e'_1} |a\rangle_{e_1} |j\rangle_{e_0} \langle b|_{e_0} \langle b'|_{e'_0}, \quad (\text{D19})$$

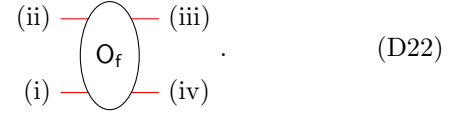
where the components of M_f can of course be expressed in terms of the components of F , B , and T . Note that we have chosen a specific ordering of the vectors in M_f . Schematically, the vectors are ordered as:



Next, we write a generic O_f in tensor component form:

$$O_f = \sum_{a', b', a, b} (O_f)_{a', b', a, b} |a'\rangle_{N'} |a\rangle_N \langle b|_N \langle b'|_{N'}, \quad (\text{D21})$$

where we have intentionally ordered the graded vectors according to the diagram:



It may be checked that with the special choices of ordering in (D20), we do not produce any Koszul signs while contracting the M_f with each other. Therefore, as suggested in section (IV B), we can simply replace all fermionic virtual legs shared by two M_f tensors with bosonic legs. Similarly, with the choice of ordering in (D22), no sign is produced in the contraction of M_f with O_f , so their common indices can also be replaced with bosonic indices. However, a Koszul sign *is* produced in the trace operation (contraction of first and last indices) due to the supertrace phase [see (7)]. However, these indices are convertible to bosonic indices with $(Z_N \otimes Z_{N'})$ -insertion (see section IV B). That is, we can replace them with bosonic indices as long as we insert an operator $Z_N \otimes Z_{N'}$ (one Z on each of the two virtual indices) before closing the MPS.

We denote the bosonic tensor obtained by replacing the fermionic virtual legs of M_f as M_b , and similarly, we denote the bosonic tensor obtained by replacing the fermionic virtual legs of O_f as O_b . Then, the state generated by M_b and O_b and $Z_N \otimes Z_{N'}$ is the same state (see Fig. 15). It is convenient to further absorb the Z factors into the definition of O_b . With this, the bMPS is generated by the tensors:

$$M_b = \sum_{\substack{j, a', a, = 0 \\ b, b'}} (M_f)_{aa', b'b}^j |a'\rangle_{e'_0} |a\rangle_{e_0} |j\rangle_{e_1} \langle b|_{e_1} \langle b'|_{e'_1} \quad (\text{D23})$$

$$O_b = \sum_{a', b', a, b} (O_f)_{a', b', a, b} (-1)^{b+b'} |a'\rangle_{N'} |a\rangle_N \langle b|_N \langle b'|_{N'}, \quad (\text{D24})$$

where the phase $(-1)^{b+b'}$ comes from the application of $Z_N \otimes Z_{N'}$. Now, contracting M_b and closing the tensor network with the bosonic tensor O_b yields $|\psi_{\text{bos}}\rangle$, and

in this way, $|\psi_{\text{bos}}\rangle$ is expressly a bMPS. Thus, we have successfully mapped the fMPS $|\psi\rangle$ to the bMPS $|\psi_{\text{bos}}\rangle$.

In summary, bosonization of a fMPS defined by a tensor \mathbf{T} and operator O_ψ as in Eq. (D2) proceeds in three steps.

1. Choose an operator $O_D = (-i\bar{\gamma})^\alpha P^\beta$ with $\alpha, \beta \in \{0, 1\}$ with which to close the bosonization TNO.
2. Construct \mathbf{M}_f by contracting \mathbf{T} , \mathbf{F} , and \mathbf{B} . Form \mathbf{O}_f by combining O_ψ and O_D .
3. Rearrange the vectors in \mathbf{M}_f and \mathbf{O}_f to match the ordering in (D20) and (D22), respectively. Form \mathbf{M}_b and \mathbf{O}_b from \mathbf{M}_f and \mathbf{O}_f by taking the graded vectors to have trivial grading and modifying the components $(O_f)_{a', b', a, b}$ of \mathbf{O}_f by $(-1)^{b+b'}$ to account for the supertrace.

In the next subsection, we provide explicit examples of the tensor network bosonization steps above.

3. Examples

We will illustrate the tensor network bosonization procedure of the previous section on two examples – a trivial atomic insulating state and the nontrivial ground state of the Kitaev chain. To motivate the TNO duality, we also analyze the examples at the operator level using the duality of section C 1.

Example 1: The trivial atomic insulating state is the ground state of the Hamiltonian $H_{\text{triv}} = -\sum_e P_e$. It has zero fermion occupancy at each site and can be expressed in the form:

$$|\psi_{\text{triv}}\rangle = \sum_{j_0, \dots, j_N} \text{tr} [T^{j_0} \dots T^{j_N} O_\psi] |j_1\rangle_{e^0} \dots |j_N\rangle_{e^N}. \quad (\text{D25})$$

with \mathbf{T} being the trivial tensor:

$$\begin{array}{c} e \\ \uparrow \\ \boxed{\mathbf{T}} \\ \leftarrow e_1 \quad \leftarrow e_0 \end{array} = |0\rangle_{e_1} |0\rangle_e |0\rangle_{e_0}, \quad (\text{D26})$$

and O_ψ equal to the parity operator P .

Using the 1D operator duality in section C 1 [Eq. (C4)], we see that H_{triv} is mapped to the spontaneous symmetry breaking Hamiltonian $H_{\text{SSB}} = -\sum_e Z_{e^1} Z_{e^0}$. In accordance, we will see that the bosonization TNO maps the ground state of H_{triv} to a ground state of H_{SSB} .

The first step of the tensor network bosonization procedure is to choose an operator O_D with which to close the bosonization TNO. For simplicity, let us choose O_D to be fermion parity P . This choice of O_D gives a map from the set of fermion parity even states to the set of states symmetric under $\prod_v X_v$ (Appendix D 1).

Next, we construct the tensor \mathbf{M}_f and the operator \mathbf{O}_f . \mathbf{M}_f is obtained by contracting \mathbf{T} , \mathbf{F} , and \mathbf{B} as in (D17):

$$\mathbf{M}_f = \mathbf{T} \cdot \mathbf{F} \cdot \mathbf{B}$$

$$\begin{aligned} &= |0\rangle_{e'_1} |0\rangle_{e'_1} \sum_{a,b} |a\rangle_{e_1} (a+b) |e\rangle_{e_0} \sum_c |c\rangle_{e_0} \langle c|_{e_0} \langle c|_{e_0} \\ &= \sum_a |0\rangle_{e'_1} \langle 0|_{e'_0} |a\rangle_{e_1} |a\rangle_{e_0} \langle a|_{e_0} \\ &= \sum_a |0\rangle_{e'_1} |a\rangle_{e_1} |a\rangle_{e_0} \langle a|_{e_0} \langle 0|_{e'_0}, \end{aligned} \quad (\text{D27})$$

and \mathbf{O}_f is simply

$$\mathbf{O}_f = \left(\sum_{b'} (-1)^{b'} |b'\rangle_{N'} \langle b'|_{0'} \right) \left(\sum_b (-1)^b |b\rangle_N \langle b|_0 \right). \quad (\text{D28})$$

Then, we rearrange the order of the graded vectors in \mathbf{M}_f and \mathbf{O}_f according to (D20) and (D22). In the final step of the tensor network bosonization procedure, we construct \mathbf{M}_b and \mathbf{O}_b by removing the grading and appropriately accounting for the supertrace. Following these steps, \mathbf{M}_b is:

$$\mathbf{M}_b = \sum_a |0\rangle_{e'_0} |a\rangle_{e_0} |a\rangle_{e_1} \langle a|_{e_1} \langle 0|_{e'_1}, \quad (\text{D29})$$

and re-ordering the vectors of \mathbf{O}_f and accounting for the supertrace gives:

$$\mathbf{O}_b = \sum_{b', b} |b'\rangle_{e'_0} |b\rangle_{e_0} \langle b|_{e_1} \langle b'|_{e'_1}. \quad (\text{D30})$$

The bosonized state is constructed by gluing together \mathbf{M}_b and closing the tensor network with \mathbf{O}_b . To see that \mathbf{M}_b generates the ground state of H_{SSB} , we first notice that, for \mathbf{M}_b in Eq. (D29), the e'_0 and e'_1 indices do not affect the bosonized state. Therefore, \mathbf{M}_b and \mathbf{O}_b can be reduced to:

$$\tilde{\mathbf{M}}_b = \sum_a |a\rangle_{e_0} |a\rangle_{e_1} \langle a|_{e_1} \quad (\text{D31})$$

$$\tilde{\mathbf{O}}_b = \sum_b |b\rangle_{e_0} \langle b|_{e_1}. \quad (\text{D32})$$

$\tilde{\mathbf{M}}_b$ generates the state:

$$|\psi_{\text{bos}}\rangle = |00\dots\rangle + |11\dots\rangle, \quad (\text{D33})$$

which is the ground state of H_{SSB} . Therefore, \mathbf{M}_b also generates the ground state of H_{SSB} .

Example 2: Now, we turn to the example of the nontrivial ground state $|\psi_K\rangle$ of the Kitaev chain. $|\psi_K\rangle$ is the ground state of the Hamiltonian $H_K = -\sum_v S_v$, and it can be written as a fMPS with [17]:

$$\mathbf{T} = \sum_{a,b} (-1)^{a(a+b)} |a\rangle_{e'_1} |a+b\rangle_e \langle b|_{e'_0}, \quad (\text{D34})$$

and $O_\psi = -i\bar{\gamma}$.

The operator duality \mathfrak{D} maps H_K to the paramagnet Hamiltonian $H_{\text{para}} = -\sum_v X_v$, so the bosonization TNO

should transform $|\psi_K\rangle$ to the paramagnet ground state $|\psi_{\text{para}}\rangle = |++\dots\rangle$, where $|+\rangle = \frac{1}{\sqrt{2}}(|0\rangle + |1\rangle)$.

Following the three steps outlined in the previous sec-

tion, we first choose O_D . Since O_ψ is fermion parity odd, we choose $O_D = (-i\tilde{\gamma})P = \gamma$. First, we compute M_f by contracting T , F , and B :

$$\begin{aligned} M_f &= T \cdot F \cdot B = \left[\sum_{a', b'} (-1)^{|b'|(|a'|+|b'|)} |a'\rangle_{e'_0} |a' + b'\rangle_{e'_1}^{C_1} (b')_{e'_1} \right] \left[\sum_{a, b} |a\rangle_{e_0} (a + b)_{e_1}^{C_1} (b)_{e_1}^{C_2} \right] \left[\sum_c |c\rangle_{e_1}^{C_2} |c\rangle_{e_1} (c)_{e_1} \right] \\ &= \sum_{a, b, a', b'} (-1)^{(b'+b)(a'+b')} \delta_{a+b, a'+b'} |a'\rangle_{e'_0} |a\rangle_{e_0} |b\rangle_{e_1} (b')_{e_1} (b')_{e'_1} \end{aligned} \quad (D35)$$

Next, we remove the grading of the vectors in M_f and $O_f = -i\tilde{\gamma}$ and account for the supertrace to form M_b and O_b :

$$\begin{aligned} M_b &= \sum_{\substack{a, b \\ a', b'}} (-1)^{(a'+b)(a'+b')} \delta_{a+b, a'+b'} \\ &\quad |a'\rangle_{e'_0} |a\rangle_{e_0} |b\rangle_{e_1} (b)_{e_1} (b')_{e'_1} \\ O_b &= \sum_{b, b'} (-1)^{b+b'} |b'\rangle_{N'} |b\rangle_N (b+1)_0 (b'+1)_{0'}. \end{aligned} \quad (D36)$$

Explicitly, we have:

$$\begin{aligned} M_b &= (|00\rangle - |11\rangle)(|0\rangle\langle 00| - |1\rangle\langle 11|) + \\ &\quad (|10\rangle + |01\rangle)(|0\rangle\langle 10| + |1\rangle\langle 01|) \end{aligned} \quad (D37)$$

$$\begin{aligned} O_b &= |00\rangle\langle 11| + |11\rangle\langle 00| \\ &\quad - |01\rangle\langle 10| - |10\rangle\langle 01|. \end{aligned} \quad (D38)$$

Defining $|v_0\rangle = |00\rangle - |11\rangle$ and $|v_1\rangle = |10\rangle + |01\rangle$ and the corresponding projectors: $P_j = |v_j\rangle\langle v_j|$, $j = 0, 1$, then M_b satisfies $M_b P_j = P_j M_b P_j$. The boundary operator also satisfies $P_j O_b = P_j O_b P_j$. Thus, there are two canonical blocks:

$$\begin{aligned} P_j M_b P_j &= |v_j\rangle\langle v_j| \quad j = 0, 1 \\ \langle v_j | O_b | v_j \rangle &= -1, \end{aligned} \quad (D39)$$

where $|+\rangle = |0\rangle + |1\rangle$. Both blocks give the same state: $-|+\rangle^{\otimes N}$.

-
- ¹ P. Jordan and E. Wigner. Über das paulische äquivalenzverbot. *Zeitschrift für Physik*, 47(9):631–651, Sep 1928.
 - ² Y.-A. Chen, A. Kapustin, and D. Radicevic. Exact bosonization in two spatial dimensions and a new class of lattice gauge theories. *ArXiv e-prints*, November 2017.
 - ³ R. C. Ball. Fermions without fermion fields. *Phys. Rev. Lett.*, 95:176407, Oct 2005.
 - ⁴ F Verstraete and J I Cirac. Mapping local hamiltonians of fermions to local hamiltonians of spins. *Journal of Statistical Mechanics: Theory and Experiment*, 2005(09):P09012–P09012, Sep 2005.
 - ⁵ Alexei Kitaev. Anyons in an exactly solved model and beyond. *Annals of Physics*, 321(1):2–111, January 2006.
 - ⁶ This is technically a C^* algebra automorphism.
 - ⁷ J. v. Neumann. Die eindeutigkeit der schrödingerschen operatoren. *Mathematische Annalen*, 104(1):570–578, Dec 1931.
 - ⁸ Jutho Haegeman, Karel Van Acoleyen, Norbert Schuch, J. Ignacio Cirac, and Frank Verstraete. Gauging quantum states: From global to local symmetries in many-body systems. *Phys. Rev. X*, 5:011024, Feb 2015.
 - ⁹ Michael Levin and Zheng-Cheng Gu. Braiding statistics approach to symmetry-protected topological phases. *Phys. Rev. B*, 86:115109, Sep 2012.
 - ¹⁰ Erez Zohar. Gauss law, Minimal Coupling and Fermionic

- PEPS for Lattice Gauge Theories. *arXiv e-prints*, page arXiv:1807.01294, Jul 2018.
- ¹¹ Tyler D. Ellison and Lukasz Fidkowski. Disentangling interacting symmetry-protected phases of fermions in two dimensions. *Phys. Rev. X*, 9:011016, Jan 2019.
- ¹² Dominic J. Williamson, Nick Bultinck, and Frank Verstraete. Symmetry-enriched topological order in tensor networks: Defects, gauging and anyon condensation. *arXiv e-prints*, page arXiv:1711.07982, Nov 2017.
- ¹³ David Aasen, Ethan Lake, and Kevin Walker. Fermion condensation and super pivotal categories. *arXiv e-prints*, page arXiv:1709.01941, Sep 2017.
- ¹⁴ Philippe Corboz and Guifré Vidal. Fermionic multi-scale entanglement renormalization ansatz. *Phys. Rev. B*, 80:165129, Oct 2009.
- ¹⁵ Philippe Corboz, Román Orús, Bela Bauer, and Guifré Vidal. Simulation of strongly correlated fermions in two spatial dimensions with fermionic projected entangled-pair states. *Phys. Rev. B*, 81:165104, Apr 2010.
- ¹⁶ Christina V. Kraus, Norbert Schuch, Frank Verstraete, and J. Ignacio Cirac. Fermionic projected entangled pair states. *Phys. Rev. A*, 81:052338, May 2010.
- ¹⁷ Nick Bultinck, Dominic J. Williamson, Jutho Haegeman, and Frank Verstraete. Fermionic matrix product states and one-dimensional topological phases. *Phys. Rev. B*, 95:075108, Feb 2017.

- ¹⁸ Nick Bultinck, Dominic J Williamson, Jutho Haegeman, and Frank Verstraete. Fermionic projected entangled-pair states and topological phases. *Journal of Physics A: Mathematical and Theoretical*, 51(2):025202, dec 2017.
- ¹⁹ Djordje Radicevic. Spin Structures and Exact Dualities in Low Dimensions. *arXiv e-prints*, page arXiv:1809.07757, Sep 2018.
- ²⁰ For each non-contractible cycle of the manifold there is an additional relation between the parity operators and hopping operators. These relations correspond to a certain product of S_e and P_f along the cycle. With an appropriate choice of η we are in the +1 sector of these relations. See [19] for more detail.
- ²¹ More formally, let v_1 be the unit tangent vector along L , in the direction of L . Then we say that the unit normal vector v_2 points to the “left” side of L if $v_1 \wedge v_2$ is equal to the orientation of the underlying 2D manifold.
- ²² Davide Gaiotto and Anton Kapustin. Spin TQFTs and fermionic phases of matter. *International Journal of Modern Physics A*, 31:1645044–184, Oct 2016.
- ²³ Note that the definition of winding number here is the winding number of the vector field relative to the normal vector of the loop L . We emphasize that this differs by a sign from a notion of the winding number of a vector field sometimes used in physics.
- ²⁴ David Cimasoni and Nicolai Reshetikhin. Dimers on surface graphs and spin structures. i. *Communications in Mathematical Physics*, 275(1):187–208, Oct 2007.
- ²⁵ Assuming the 2D fPEPS is defined on a triangulation of an orientable 2D manifold.
- ²⁶ Yu-An Chen and Anton Kapustin. Bosonization in three spatial dimensions and a 2-form gauge theory. *arXiv e-prints*, page arXiv:1807.07081, Jul 2018.
- ²⁷ Wilbur Shirley, Kevin Slagle, and Xie Chen. Foliated fracton order from gauging subsystem symmetries. *SciPost Phys.*, 6:41, 2019.
- ²⁸ Aleksander Kubica and Beni Yoshida. Ungauging quantum error-correcting codes. *arXiv e-prints*, page arXiv:1805.01836, May 2018.
- ²⁹ Alexei Kitaev and Chris Laumann. Topological phases and quantum computation. *arXiv e-prints*, page arXiv:0904.2771, Apr 2009.